The Thesis Committee for Pinar Goktas
Certifies that this is the approved version of the following thesis:

Morphologies and controls on development of Pliocene-Pleistocene carbonate platforms: Northern Carnarvon Basin, Northwest Shelf of Australia

APPROVED BY
SUPERVISING COMMITTEE:

Supervisor:

Craig S. Fulthorpe, Supervisor

James A. Austin Jr., Supervisor

Ronald J. Steel

William L. Fisher

Morphologies and controls on development of Pliocene-Pleistocene carbonate platforms: Northern Carnarvon Basin, Northwest Shelf of Australia

by

Pinar Goktas, B.Sc.

Thesis

Presented to the Faculty of the Graduate School of

The University of Texas at Austin

in Partial Fulfillment

of the Requirements

for the Degree of

Master of Science in Geological Sciences

The University of Texas at Austin

August 2013

Dedication

This thesis is dedicated to my family Orhan, Suheyla and Yigit and my fiancé Kerem for their endless support and encouragement.

Acknowledgements

There years ago, I received a very warm welcome from Bill Fisher who was the first person I met in the Jackson School of Geoscience. Fortunately, this warm welcome continued when I meet with my great supervisors, Craig Fulthorpe and Jamie Austin. Their trust and enthusiasm never ceased during the last two years, and without their patient and professional approach this thesis would never have been achievable. Besides their scientific support, their kindness and overwhelming encouragement made my last two years unforgettable. I am also indebted to my committee member, Ronald Steel for his great support, valuable time and suggestions. In addition, I have learned from the many professors and researchers at the UT Department of Geological Sciences and Institute of Geophysics during the course of this research.

Without Turkish Petroleum Corporation's financial support I would never be able to get this education and these experiences. Also, I would like to thank UTIG and BEG technical support, especially to Dallas Dunlap for his valuable time and promptness in solving my problems.

I am grateful to my colleague friends Marina, Maurine and Jason who have shared experiences in our office until late office hours even weekends. Last but not least are my family and outside of school friends. I would like to thank Kerem Tozun who always listened and encouraged me to keep going last three years, and kept motivated for our future. I am grateful to my mother, father and brother for giving much encouragement and endless support and for teaching me how to stand on my own two feet.

Abstract

Morphologies and controls on development of Pliocene-Pleistocene carbonate platforms: Northern Carnarvon Basin, Northwest Shelf of Australia

Pinar Goktas, MSGeoSci

The University of Texas at Austin, 2013

Supervisors: Craig S. Fulthorpe and James A. Austin Jr.

The detailed morphologies, evolution and termination of Neogene tropical carbonate platforms in the Northern Carnarvon Basin (NCB) on the passive margin of the Northwest Shelf of Australia reveal information on the history of local oceanographic processes and changing climate. Cool-water carbonate deposition, dominant during the early-middle Miocene, was superseded by a siliciclastic influx, which prograded across the shelf beginning in the late-middle Miocene during a period of long-term global sea-level fall. The resulting prograding clinoform sets, interpreted as delta lobes, created relict topographic highs following Pliocene termination of the siliciclastic influx (Sanchez et al., 2012a; 2012b). These highs created a favorable shallow-water environment for subsequent photozoan carbonate production. A composite, commercial 3D seismic volume allows investigation of the temporal and spatial evolution of the resulting Pliocene-Pleistocene carbonate platforms. Initiation of carbonate development, in addition to being a response to cessation of siliciclastic influx and the existence of suitable shallow-water substrate, was also influenced by the development of the warm-

water Leeuwin Current (LC), flowing southwestward along the margin. Four flat-topped platforms are mapped; each platform top is a sequence boundary defined by onlap above and truncation below the boundary. Successive platforms migrated southwestward, along-strike. Internally, platforms have progradational seismic geometries. The mapped platform tops are large (≥ 10 km wide). Evidence of karst (e.g., v-shaped troughs up to 50m deep and ~1 km wide and broader karst basins up to 20 km^2 coverage area) on platform tops suggests episodic subaerial exposure that contributed to the demise of individual platforms. The most recent platform, platform 4, is unique in having interpreted reefs superimposed on the progradational platform base. The base of these reefs now lies at ~153 m and the reefs may therefore have developed post-LGM (~21 Ka). The reefs subsequently drowned, with drowning possibly aided by turbidity associated with formation of adjacent sediment drifts and weakening and strengthening LC during the late Pleistocene. The progressive drowning and termination of platforms from northeast to southwest along strike may result from differential compaction of the deltaic substrate or differential tectonic subsidence caused by the collision at the Banda Arc between the Australian and Pacific plates.

Table of Contents

List of Figures

Chapter 1: Introduction

1.1 INTRODUCTION

Sequence stratigraphic models have been used for decades to understand the factors controlling sedimentary facies generated by relative sea-level change and other forcing factors like changes in sediment supply, and to predict facies distributions to reconstruct depositional setting and paleogeography. Response to changes in base level, including the surfaces created in response to relative sea-level changes, can be similar in both clastic and carbonate systems. However, sediment production in carbonate successions is more sensitive to local/*in-situ* processes associated with environmental conditions, such as light level/water clarity (affecting photosynthesis) and water depth, as well as water temperature and chemistry, that do not influence siliciclastic sediment production (Kendall and Schlager, 1981; Catuneanu et al., 2011). Furthermore, while carbonate sediment deposition, diagenesis, lithification and preservation are sensitive to base-level fluctuations, carbonate platform geometry is also affected by wind direction and ocean currents that shape biogenically-driven sedimentation patterns (Isern er al., 2004; Kendall and Schlager, 1981).

Carbonate sequences and parasequences have generally been interpreted to result from external forcing, particularly by changes in relative sea level. Autocyclic processes, such as delta switching or lateral migration of beach-barrier bars, have usually also been considered significant controls on carbonate sequences. Comparing morphologies and sedimentary processes (i.e., channel-levee complexes; Mulder and Syvitski, 1995) in carbonate systems and their siliciclastic counterparts suggest that carbonate systems are

more complicated and include complex sedimentary morphologies, some of which have not been well-studied yet (Mulder and Syvitski, 1995).

In addition to global sea level and climate changes, deep earth processes may play a role in carbonate depositional system/coral reef evolution (DiCaprio et al., 2010). For example, mantle flow is hypothesized to affect rates of dynamically driven subsidence beneath the northeast Australian margin and is therefore thought to have influenced the development of the Great Barrier Reef (GBR). Determining the rate of subsidence from the GBR would in turn place a regional constraint on the interaction between plate motion and mantle convection (DiCaprio et al., 2010). Carbonate platforms on the Northwest Shelf (NWS) of Australia formed in a similar passive margin setting to those of the GBR (DiCaprio et al., 2010) and have similar seismic geometries (Sanchez, 2011), suggesting similar control mechanisms. These passive margin carbonates are not yet well understood, but could provide facies models that would be valuable for interpreting the older rock record (James et al., 2004).

This research documents the temporal and spatial evolution of seismically interpreted Pliocene-Pleistocene carbonate platforms in the Dampier Sub-basin of the NWS. We link the observed geometries and distribution of these buildups, interpreted using composite commercial 3D seismic volumes, to possible local/regional processes responsible for their development. This work builds on previous research that has documented the earlier (late Oligocene-Pleistocene) stages of the development of this mixed siliciclastic and carbonate margin (Cathro, 2002; Liu et al., 2011; Sanchez, 2011; Sanchez et al., 2012a; 2012b). Sanchez (2011) first inferred the existence of buried Plio-Pleistocene photozoan carbonate platforms based on their seismic architectures. Sanchez (2011) further suggested that these platforms developed on top of relict highs created by underlying, upper Miocene-Pliocene siliciclastic delta lobes (Sanchez et al, 2012a;

2012b), and that their asymmetric platform geometries were influenced by the Leeuwin Current (LC).

Interpretation and mapping of 3D seismic data in this region enables us to propose a model for the evolution of four of these buried platforms and to constrain more completely processes involved in their initiation, morphologic evolution and termination. Additional goals are to investigate the competing roles of paleoenvironmental factors, including relative sea level changes, sediment supply and known regional tectonism, on platform development.

The NWS is a late Paleozoic, Mesozoic and Cenozoic sedimentary succession developed following the breakup of Gondwana (Exon and Colwell, 1994; Longley & Bradshaw, 2001). The NWS is divided into separate basins: the Northern Carnarvon, Roebuck, Offshore Canning, Browse and Bonaparte (Longley & Bradshaw, 2001). The region is bounded by the Australian craton to the east and south and by Mesozoic oceanic crust to the north and west (Fig. 1.1).

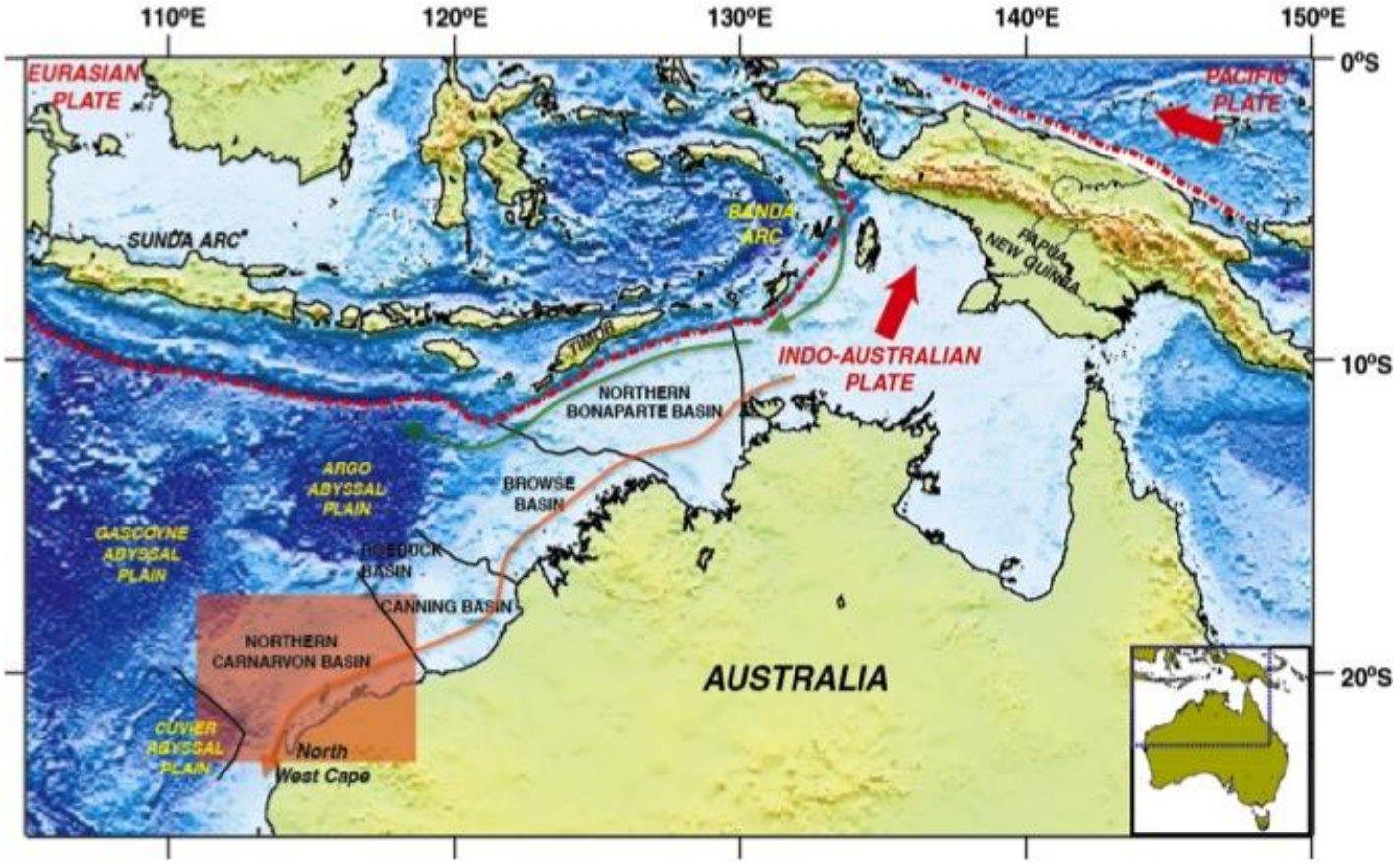

Figure 1.1: The Australian Northwest Shelf (NWS) and component basins: Carnarvon, offshore Canning Roebuck, Browse and Bonaparte basins. The red box over Northern Carnarvon Basin highlights the study area shown in Fig.1.2. Inset map shows the location of the NWS with respect to the Australian continent. The orange arrow shows the general path of the Leeuwin Current (LC), which flows along the Western Australia shelf edge, and the green arrows shows the Indonesian Throughflow (ITF; modified after Cathro, 2002).

The Carnarvon Basin is elongated northeast-southwest and its offshore component covers >500,000 km^2 in water depths of up to 3500 m. The basin contains a maximum thickness of 15 km. of Triassic-Early Cretaceous siliciclastic deltaic to marine deposits and Mid-Cretaceous-Cenozoic slope and shelfal marls and carbonates (Longley & Bradshaw, 2001). The Northern Carnarvon Basin (NCB) is in turn divided into sub-basins and structural highs defined by north-northeast trending basin faults (Fig 1.2; Karner and Driscoll, 1999). Development of sub-basins was controlled by successive periods of extension and thermal subsidence (Karner and Driscoll, 1999). This study focuses on the Dampier Sub-basin of the NCB (Fig. 1. 2).

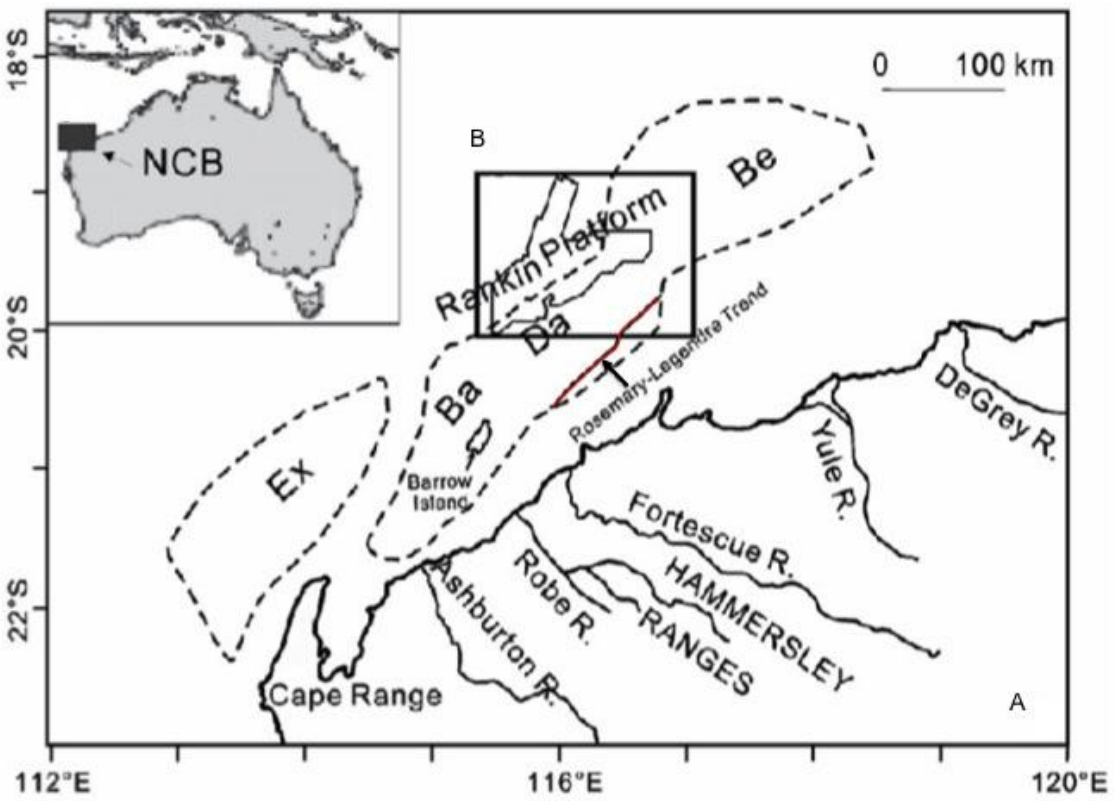

Figure 1.2: Mesozoic sub-basins of the Northern Carnarvon Basin (outlined by black dashed lines): Exmouth (Ex), Barrow (Ba), Dampier (Da) and Beagle (Be) (Romine et al., 1997; Cathro et al., 2003), and available 3D seismic data (irregular polygon within black rectangle, our detailed study area) in the Dampier sub-basin and across the Rankin Platform. The red line shows the Rosemary-Legendre (RLT), a localized Miocene inversion structure trend created by collision of Australia and the Indonesian arc (Karner and Driscoll, 1999). The modern terrestrial drainage system is also shown (Semeniuk, 1996). Inset map shows the general location of the study area on the northwest margin of Australia.

The NWS is an important hydrocarbon province. Exploration in the offshore Dampier Sub-basin dates back to 1968 with the Legendre 1 oil discoveries (Longley & Bradshaw, 2001). Since that time until ~10 years ago, ~754 wells have been drilled and 145 GL of oil, 52 GL of condensate and 207 BCM of gas have been produced (Longley & Bradshaw, 2001). Remaining known reserves are 76 GL of oil, 93 GL of condensate and 604 BCM of gas. Almost all hydrocarbon resources are in Upper Triassic, Jurassic and Lower Cretaceous sandstones (Longley & Bradshaw, 2001).

1.2 PREVIOUS WORK

Because of the complexity and heterogeneity of interpreted carbonate buildups on the NWS, interpretation using 2D seismic profiles has been increasingly superseded by interpretation of 3D seismic data. Indeed, the use of 3D images has revolutionized our view of stratigraphic successions, and in particular complex carbonate platforms. Plan-view images involving amplitude extraction reveal features, particularly discontinuities, that cannot be observed using 2D profiles (Liu et al., 2011). Mapping of platform external morphology and internal architectures using 3D seismic data documents both spatial and temporal changes and allows investigation of factors involved in shaping the platforms, including relative sea level changes, paleoenvironment and paleoceanography, depositional/erosional processes and subsidence rate, including both tectonic subsidence and differential compaction.

Worldwide, 3D data have been used to define carbonate platform structural features and stratigraphically important seismic horizons, reconstruct platform development, and identify of the main controls on platform evolution (Zampetti et al, 2004; Fournier et al., 2005; Colpaert et al., 2007). For example, hydrocarbon recovery from the prograding shoal complex of the Permian Kluff Formation, Oman, has been

improved by applying structure-oriented filtering (SOF), which is only possible using 3D images. Background noise has also been removed, leading to improved imaging of mounded continuous/discontinuous, progradational shingle and progradational sigmoidal structures *en route* to development of an improved depositional model (Masaferro et al., 2003). In another Oman study, Upper Cretaceous ramp-type carbonate reservoirs have been delineated using 3D time slices, image-filtering reflectivity and combined volume dip azimuth techniques (Masaferro et al., 2003). In addition, porosity distribution has been estimated from the acoustic impedance volume, to develop a reservoir model (Fournier et al., 2005). Another application of 3D interpretive techniques has been used in connection with a middle Miocene, isolated build-up in the Luconia Province, offshore Sarawak, Malaysia. Using the root mean square (RMS) method, mounded reef seismic facies are extracted by applying a definite amplitude window. Higher output amplitude values correspond to the reef facies, allowing them to be mapped through the entire seismic volume. Both reef tracts and onlapping back-reef facies have been distinguished (Zampetti et al., 2004). Finally, in the Malampaya Field, Philippines, body-checking has been applied. This method defines numerous levels of seismic discontinuities based on different amplitude thresholds. Different colors represent wavelets forming in the geobody (Davies et al., 2004).

Use of 3D seismic data to study the Cenozoic section in the NCB began with detailed mapping of late Paloegene-Neogene clinoformal sequences by Cathro and Austin (2001), Cathro (2002) and Cathro et al. (2003). Geologic age estimates for the mapped sequences were provided using analyses of sidewall cuttings by Moss et al (2004), who analyzed Eocene-Pliocene biostratigraphy of the Dampier Sub-basin. In the same general area, the early-middle Miocene- Pleistocene age interval was studied by Liu et al (2011)

and Sanchez (2011, 2012a; 2012b), using a larger 3D volume that incorporated, and expanded beyond, that of Cathro et al. (2003; Fig. 1.3).

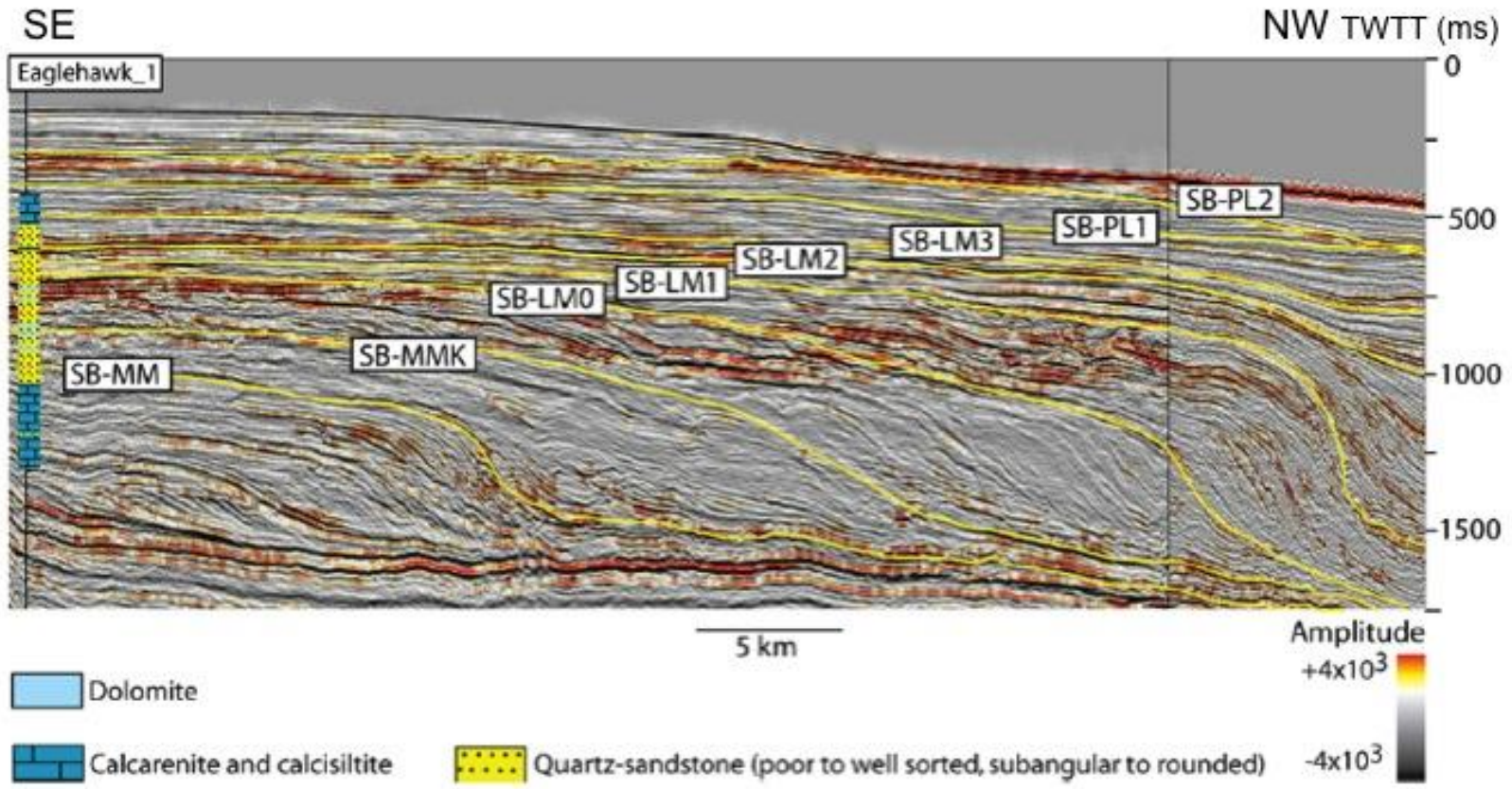

Figure1.3: Dip-oriented seismic profile showing early-middle Miocene to Pliocene sequence boundaries interpreted by Sanchez (2011) and Liu et al (2011), and a correlation with lithologies from the Eaglehawk_1 industry well (Moss et al., 2004).

Studies of Pliocene-Quaternary reef development on the NWS have been limited. Research has focused on modern carbonate platform morphology and its response to sea level changes and oceanographic processes (Collins et al., 2002). Sanchez (2011) identified similar platforms in the subsurface for the first time. Building upon initial mapping by Cathro (2002), Sanchez (2011) identified six large (≥10 km across) buried carbonate platforms of Pliocene-Pleistocene age. These platforms were presumed to comprise photozoan carbonates deposited in shallow water, based on their flat-topped morphologies, which indicate growth to near sea level (Fig. 1.4). Sanchez (2011) also documented the internal, asymmetric progradational seismic geometries within these platforms and ascribed them to the influence of sea-level change and ocean currents. The platforms were not contemporaneous, but migrated southwestward along margin strike (Fig. 1.4). They appear to have formed on top of late-middle to late Miocene-age delta lobes of the siliciclastic Bare Formation that had migrated in the opposite direction, northeastward; (Fig. 1.4). Sanchez (2011) proposed that the initiation of the Leeuwin Current (LC, Fig. 1.1) caused the seismically observed transition from northeastward-directed delta lobe migration to southwest-directed migration of the overlying Pliocene-Pleistocene carbonate platforms.

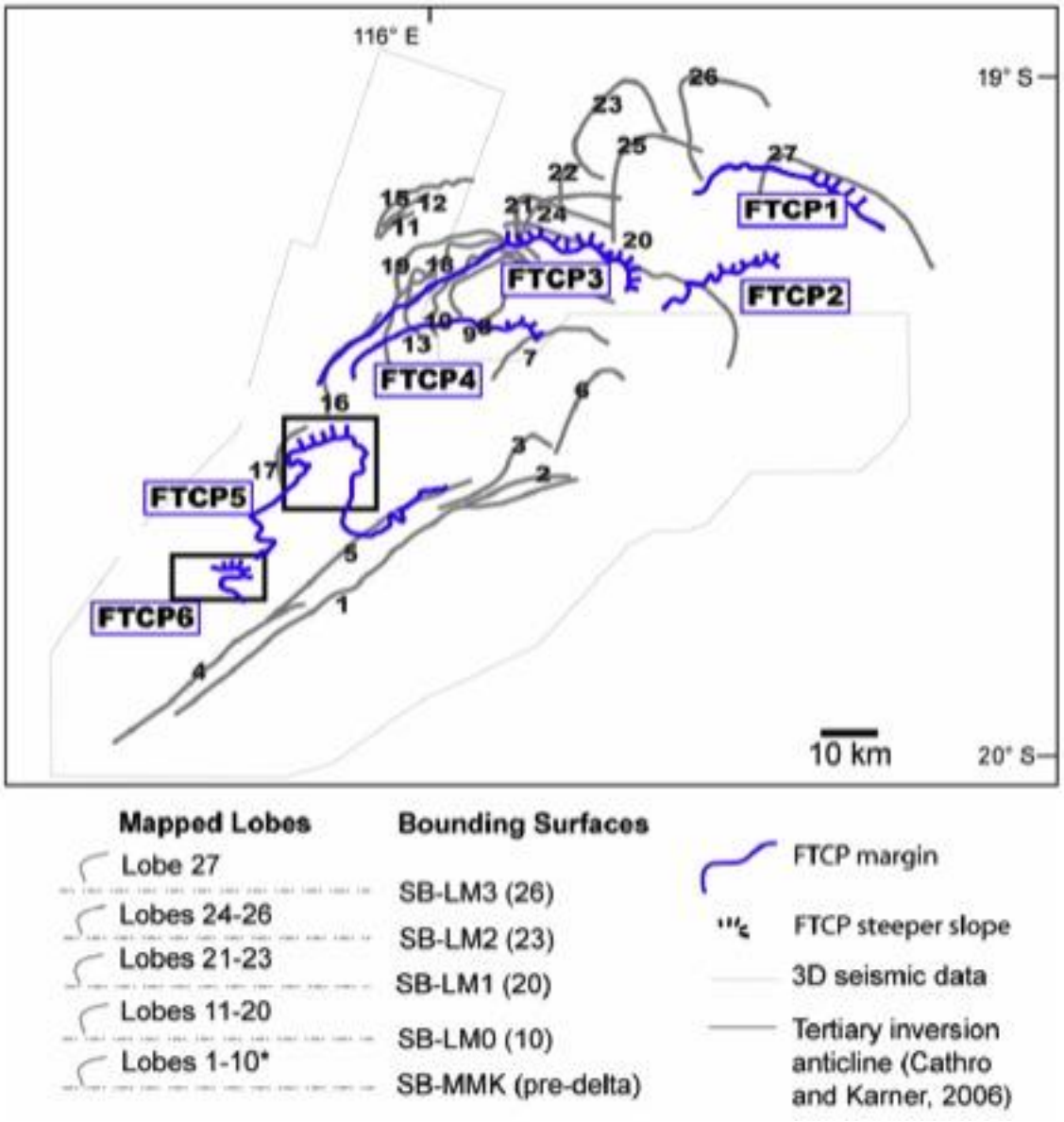

Figure 1.4: Six "flat-topped carbonate platforms" (FTCP 1-6; marked by blue lines) interpreted by Sanchez (2011). Note that platforms appear to have evolved above older topographic highs/deltaic depocenters (indicated by grey lines with deltaic lobes numbered 1-27).

1.3. OBJECTIVES AND SIGNIFICANCE

The research described here involves more detailed seismic interpretation of four of Sanchez's (2011) carbonate platforms (Fig. 1.5). Platform 3 and Platform 4 of this study are identical with FTCP5 and FTCP6 of Sanchez (2011; Fig. 1.4). FTCP3 of Sanchez (2011), interpreted using both 2D and 3D data, constitutes part of our Platform 2. Platforms 1-3 are all buried platforms. In contrast, our Platform 4 is newly identified and is exposed at and above the seafloor.

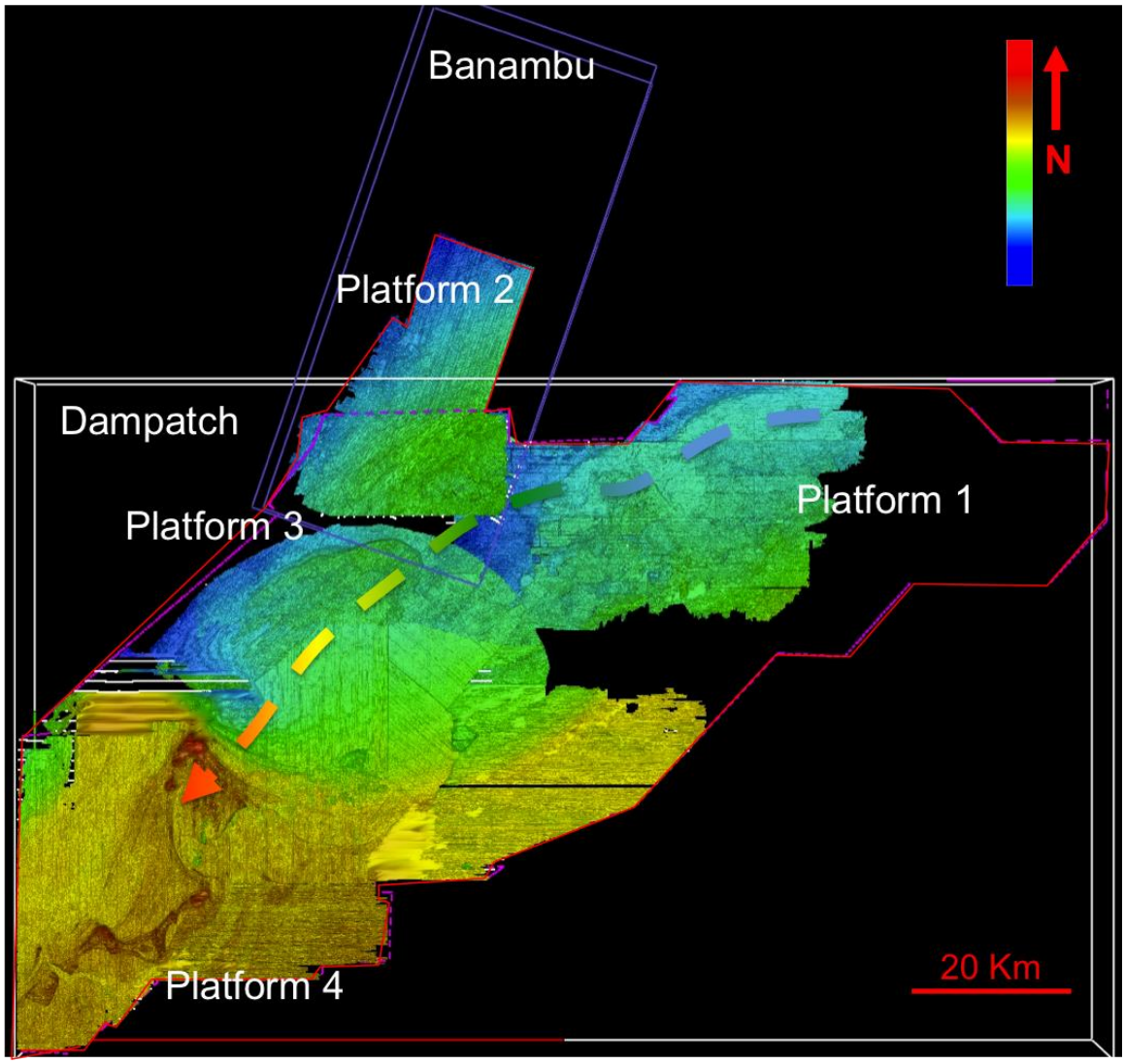

Figure 1.5: Mapped tops of platforms 1-4. The colored arrow illustrates the age progression of the platforms, from oldest (Platform 1) to youngest (Platform 4)

Platform tops are well defined by high-amplitude reflections that are ideal for making maps and cross-sections that are crucial for paleo-morphological reconstructions. The maps and profiles together provide evidence suggesting subaerial exposure of platform tops and patterns of progradation. We concur with Sanchez (2011) that the available seismic evidence suggests both platform evolution and drowning in response to relative sea-level changes. As also noted by Sanchez (2011), the platforms have relatively flat tops; internal clinoforms dip asymmetrically in 3D, suggesting spatial differences in the intensity of waves and/or current affecting the platforms. Irregularities on platform tops, observed in both profile and map views, are similar to those interpreted by Cathro and Austin (2001).

This study builds on that of Sanchez (2011) by mapping the platforms employing the full potential of the 3D data to conduct a seismic geomorphological interpretation. Furthermore, in contrast to Sanchez (2011), who interpreted the tops of all platforms as flooding surfaces, we interpret the tops of platforms 1, platform 2 and 3 together as sequence boundaries, as these tops are generally characterized by reflector terminations both above and below. The top of platform 4 is the modern seafloor.

We investigate three possible processes proposed by Sanchez (2011) for the initiation and demise of photozoan platforms on the NWS: 1) Arid climate conditions shut off siliciclastic input to the outer shelf during the Pliocene, allowing reef and biogenic platform development; 2) Strengthening of the SW-directed LC in the Pliocene-Pleistocene created more favorable environmental conditions for reef/platform development (i.e., higher nutrient contents and warmer water temperatures; Gallagher et al., 2009); 3) Platform drowning and observed NE to SW along-strike migration resulted from differential subsidence linked to compaction of the underlying siliciclastic delta lobes. As hypothesized by Sanchez (2011), this differential subsidence may have been

caused by platform loading and/or plate deformation caused by ongoing collision between Australia and the Banda Arc (Collins et al., 2002).

Chapter 2: Geological Background

2.1.TECTONIC HISTORY

The NCB has been shaped by the progressive and ongoing break-up of the Gondwana supercontinent (Hull and Griffiths, 2002). The NWS developed in response to three distinct rifting phases, from the Late Permian to early Late Cretaceous. Tectonism began with extension of the Carboniferous-Permian intracratonic Westralian Superbasin (Cathro & Karner, 2006). Subsequently, Triassic-Cretaceous rifting and Early Cretaceous thermal subsidence, punctuated by minor structural inversions, led to development of the modern sub-basins of the NCB (Exmouth, Barrow, Dampier and Beagle), together with the Rankin Platform (Figs. 1.2 and 2.1; Bradshaw et al., 1988)

Separation of Australia and Antarctica represents the final stage of relocating the north-south axis from the Indian Ocean to the Southern Ocean resulted from Paleogene collision of Greater India and the Eurasian Plate (Miller et al., 1991). Seafloor-spreading within the Indian Ocean and the Southern Ocean has caused net northward movement of Australia since the Oligocene (Hull and Griffiths, 2002). In the early Miocene, the northward-moving Australian continent began to collide with a series of island arcs on the southern edge of the Eurasian Plate, the Banda Arc (Fig. 1.1). During the same interval, the westward-moving Pacific Plate came into contact with the Australasian Plate. The result of these plate interactions has been to create an anti-clockwise rotation of the Australian continent. Resultant torque has led to buckling of the North Australian lithosphere and dextral, transcurrent movement along preexisting fractures near the continent-ocean boundary on this part of the Australian continent (Veevers and Powell, 1984).

A by-product of the collision of the Australasian Plate with the Banda Arc/Indonesia (Veevers et al., 1991, Karner and Driscoll, 1999, Hull and Griffiths, 2002) has been late Miocene-Pliocene reactivation of the Rosemary-Legendary structural trend, involving uplift of up to 75 m., and accelerated subsidence of the area basinward of the Rosemary Fault (Hull and Griffiths, 2002; Cathro and Karner, 2006).

Well-developed, prograding Oligocene to mid-Miocene clinoformal sedimentary sequences are mainly eustatically controlled, but the ongoing Banda Arc collision has tectonically deformed late Miocene-Recent sequences (Cathro et al., 2002; Cathro and Karner, 2006). For example, accelerated subsidence occurred during this time in the Dampier Sub-basin. However, unlike the Madeline and Legendre trends, the Rankin Platform subsided homogeneously as a rigid block (Hull and Griffiths, 2002). Therefore, although the NWS is a fundamentally a passive margin, tectonism has a continuing, though limited, impact on the region

2.2 SEDIMENTARY HISTORY

While tectonism has driven basin development on the NWS and continues to cause local deformation, climate has been the most important control on sediment type in this region. The NWS has moved northward from ~40°S to ~20°S since the Eocene (Apthorpe, 1988; McGowran et al., 1997), causing a long-term paleoclimate trend towards warmer and more arid conditions and enhancing shelfal carbonate production. The result has been a transition from a Mesozoic siliciclastic succession to predominantly carbonate sedimentation since the Eocene on the NWS (Apthorpe,1988; Butcher, 1989).

The first facies subdivision by Heath and Apthorpe (1984) for the offshore Cenozoic carbonate basins of the NWS has been improved by several subsequent studies using well data. Cenozoic carbonates of NWS were divided by Wallace et al. (2003) into

five major water-depth dependent facies: Paleocene-Eocene basinal, Oligocene-Miocene slope-canyon, Oligocene-Miocene shelf facies, Oligocene-Quaternary nearshore and Pliocene-Quaternary shelf. The upper Oligocene-early upper Miocene heterozoan carbonate succession comprises primarily seismically well-imaged, northwest-directed prograding clinoforms, with slope inclinations of 2-8°. Cathro et al. (2003) have argued that the associated paleo–shelf edges were always submerged at depths of 20-200 m., even at lowstands. Two Oligocene-middle Miocene formations have been defined by Heath and Apthorpe (1984) based on offshore well data: the Mandu Formation and Tulki Limestone (Fig. 2). The Mandu Formation is a sandy limestone formed in the early late Oligocene-early Miocene and represents a shallowing-upward sequence (Butcher, 1989). Apthorpe (1988) has interpreted the younger Tulki Limestone as a low-angle, cross-bedded clastic carbonate succession deposited on shoals or banks. The Trealla Limestone, a middle Miocene bioclastic calcerinite, overlies the Mandu and Tulki formations. Heterozoan carbonate development was dominant by the Eocene, but was interrupted by the shallowing upward, dolomitic, siliciclastic sands of the late-middle to late Miocene Bare Formation (Butcher, 1989). The Bare Formation has recently been interpreted as a system of deltas fed by rivers in a tropical-semi desert environment (Cathro, 2002; Sanchez et al., 2012a; 2012b). Sanchez et al. (2012a, 2012b) have pointed out that this formation correlates with similar Miocene siliciclastic influxes worldwide, and have further hypothesized that this siliciclastic influx resulted from long-term global sea-level fall and global cooling, along with presumed increased erosional rates from the adjacent Australian continent.

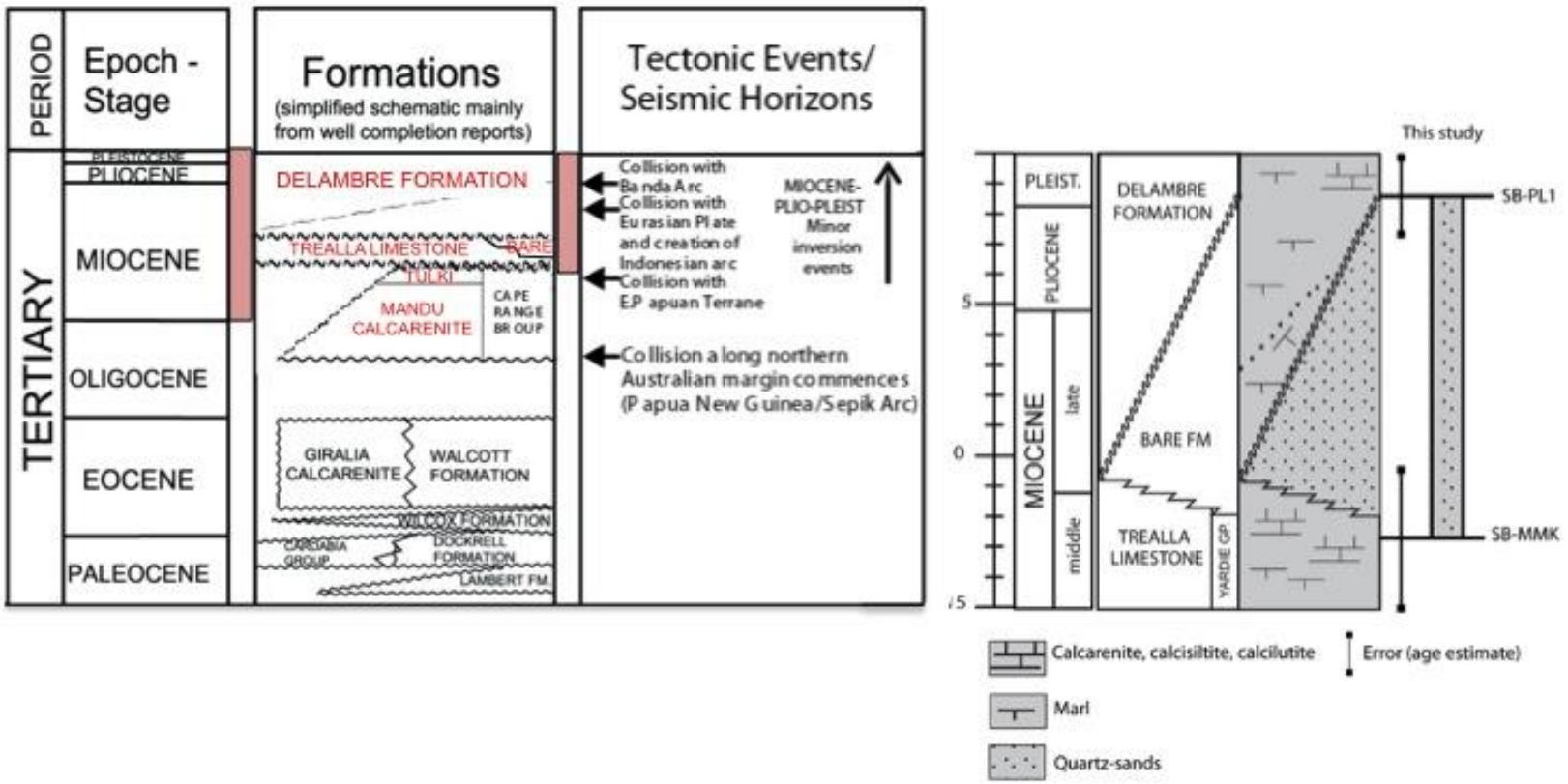

Figure 2: Generalized Tertiary stratigraphy and tectonic events on the NWS. Miocene-Pleistocene stratigraphy is derived from Berggren et al. (1995). Sequence boundaries (SB-MM1, SB-PL1) have been defined by Sanchez (2011). SB-PL1 is the base of the interval which includes the carbonate platforms described in this work (Modified from Cathro, 2002; Sanchez, 2011).

In general, the succession from the Paleocene to the late Miocene displays a shallowing-upward trend. This trend was interrupted by a major transgression in the early Pliocene, which created more open shelf conditions and deposition of pure limestone (Wallace et al., 2003). Pliocene-Quaternary shelf facies comprise uncemented, coarse-grained limestone, comprising foraminifera, echinoderms, bivalves and peloids (Wallace et al., 2003). Data acquired from the Finucane-1 and Bounty-1 wells indicate that this interval is equivalent to the Delambre Formation, the top of which is the modern seafloor (Heath and Apthorpe, 1984; Butcher, 1989). The presence of tropical large foraminifera indicates an open marine environment in water depths shallower than 130 m (Wallace et al., 2003).

2.3 OCEANOGRAPHIC SETTING

Currents exert a significant influence on NWS sedimentation. Major controls on ocean circulation are the Indonesian Throughflow (ITF) (Fig. 1.1), the LC, and tides, swells and wind regimes. The LC is an unusual south-flowing eastern boundary current and flows in the opposite direction to the modern prevailing wind direction. The LC has a significant effect on climate of NWS (James et al., 2004; Sanchez, 2011).

Upwelling and long-shore winds are overwhelmed by upper-ocean (upper 250-300 m.) pressure gradients as the driving mechanisms for the LC (Sinha et al., 2007; Pattiaratchi, 2004). The ~0.5 m height difference between the less dense and low salinity Timor Sea and cooler, denser, saline water off the coast of the Perth interaction induce the LC, which is <100 km. wide and < 300 m. deep) (Pattiaratchi, 2004). The pressure gradient created leads to easterly flow of central Indian Ocean subtropical water towards the Australian coast at 15°-35° S latitude. The LC is formed by deflection of this easterly flow to the south (Figs. 1.1).

The timing of LC initiation has long been debated. McGowran et al. (1997) drew on observed patterns of biogenic carbonate production to suggest that the LC initiated in the middle Eocene as a result of the separation of Australasia and Antarctica, which allowed warm oceanic circulation to the southwest. They explained periods of LC inactivity during the late Paleogene and Neogene as the result of patterns of major transgression and global cooling.

More recently, Gallagher et al. (2009), based on foraminiferal sediment distribution, have argued for ITF connectivity and LC initiation 10 Ma. In contrast to McGowran et al. (1997), Gallagher et al. (2009) have proposed that observed fluctuations in the abundance of Indo-Pacific taxa were linked to relative restriction of connectivity between the Indian and Pacific oceans. For example, the lack of Indo-Pacific taxa on the NWS from 10-4.4 Ma is ascribed to such restriction of connectivity. A relative lack of Indo-Pacific taxa from 4.4-1.6 Ma also suggests constriction of ITF or non-connectivity, which is associated with aridification and cooling in the Indian Ocean and Africa (Gallagher et al. 2009). Indo-Pacific taxa become abundant after 1.6 Ma, during the middle Pliocene climatic transition, because of improved connectivity with the West Pacific Warm Pool (WPWP), which corresponds with stronger and warmer ITF and initiation of the modern oligotrophic LC (Gallagher et al. 2009). A subsequent reduction in Indo-Pacific taxa at 0.8 Ma correlates with the initiation of large glacial/interglacial oscillations (100 ky. cycles) and Indonesian uplift, which together restricted the seaway.

Understanding fluctuations in the strength of the LC during the Pliocene, Pleistocene and Holocene, which include evident ocean circulation changes caused by waxing and waning of ice sheets, reveal the importance of opening ocean geometries on current development during the late Neogene (Sinha et al., 2007). Karas et al. (2011) have used planktonic foraminiferal $\delta^{18}O$ and Mg/Ca ratios to show that sea surface

temperatures (SST) fell across the subtropical Indian Ocean during the Pliocene. They have also proposed that this SST lowering was associated with a tectonically reduced ITF. Sinha et al (2007) has applied stratified isotopic records of surface-dwelling and thermocline-dwelling planktonic species from the Miocene/Pliocene transition to the Pleistocene to characterize LC strength. Sinha et al (2007) and Karas et al. (2011) conclude that the LC initiated at 2.5 Ma, which helps to explain the genesis and evolution of the non-contemporaneous carbonate platforms targeted in this investigation.

Chapter 3:Data And Methodology

3.1 DATA

The seismic data were acquired during petroleum exploration in the NCB and donated to the University of Texas Institute of Geophysics (UTIG) by Woodside Petroleum, Ltd. The 3D seismic data are a merged volume covering 7,500 km^2, comprising surveys acquired during the 1980s and 1990s and located on the Rankin Trend northwest of the Dampier Sub-basin (Fig. 3).

No wireline logs cover the shallow sub-seafloor interval (<500 ms TWTT) on which this study focuses. However, assuming an average velocity of 4,000 m/s for such carbonate lithologies (Schlager, 2005) and using a central frequency for the available 3D seismic data of ~55 Hz, vertical resolution is calculated to be ~18 m within this interval (Sanchez, 2011).

Age control is also limited because the late Neogene section studied here has not been considered prospective for hydrocarbons (Cathro, 2002). Age estimates that do exist are derived from a foraminiferal biostratigraphic analysis of samples from four wells in the study area (Moss et al., 2004).

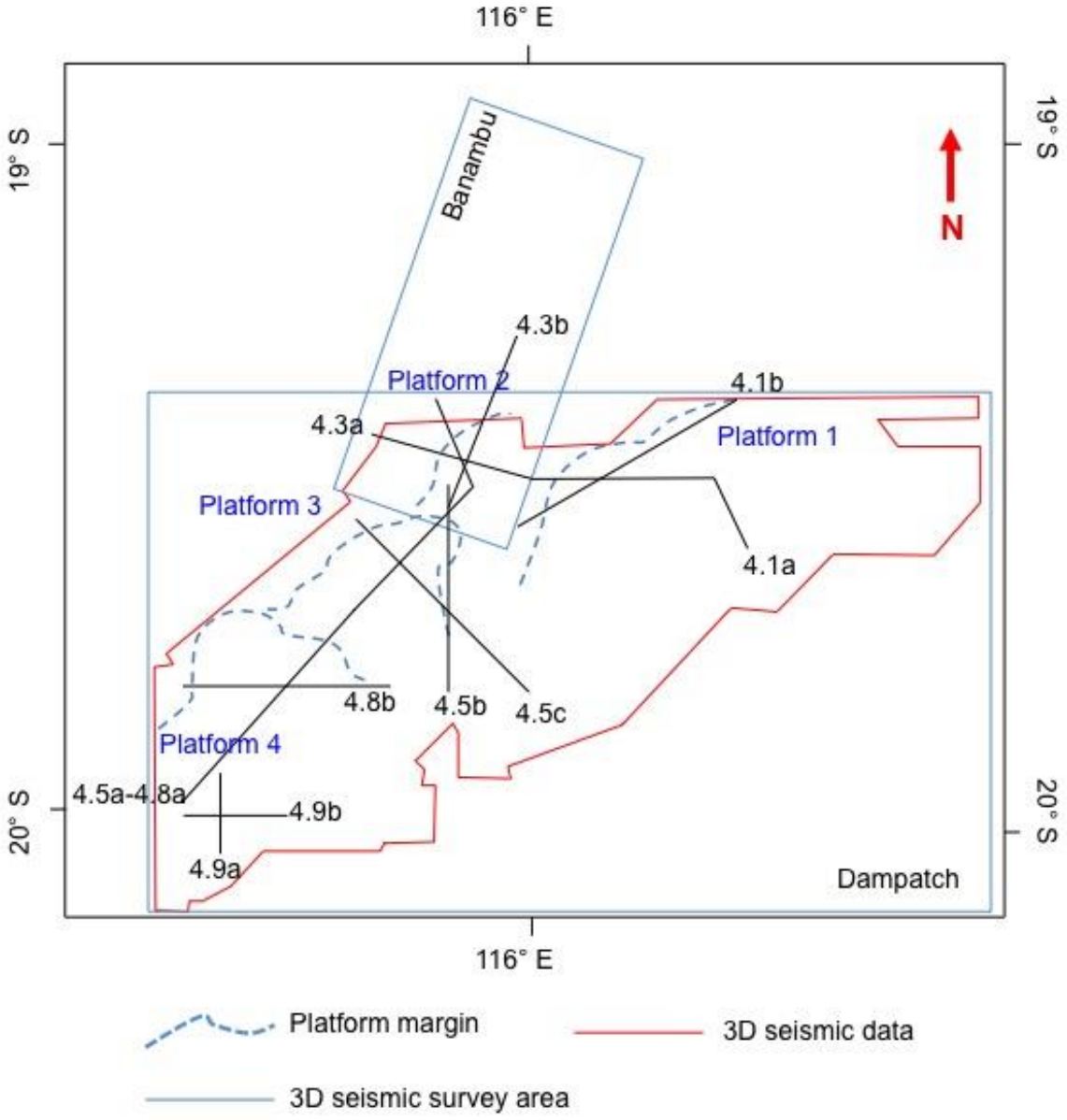

Figure 3: The two separate 3D seismic surveys used for this project: the Dampatch merged volume and the Banambu. The total area covered by both volumes is ~7500 km^2. Also shown are outlines and steep-side margin of interpreted platforms 1-4 and the locations of seismic profile images shown.

3.2 METHODOLOGY

Key seismic facies, discontinuities, downlap and onlap surfaces within the interpreted/mapped Pliocene-Pleistocene carbonate platforms are examined using profile views, mapped horizontal time slices and mapped interpreted horizons within the 3D seismic volume. The 3D data are loaded onto a DecisionSpace® workstation available at UTIG for interactive interpretation. Using the DecisionSpace® attribute generation application, a reflection attribute is generated in the time domain with a 32-bit sample size and a window of 17 samples. An underlying assumption of generating such reflection amplitude volumes is that the seismic waveform expression and reflection character of the carbonate platforms differ from those of the neighboring sediment. Sequence boundaries are then identified based on onlap by overlying sediment and truncation of underlying sediment.

Horizon or surface maps are useful for evaluating the influence of oceanographic processes in shaping the platforms. Time slices reveal high variance, such as occurs at reefs or unconformities (Zampetti et al., 2004). Horizontal time slices are then generated, spaced ~4 ms apart in the interval from 16-420 ms. Reflection amplitude extractions illustrate the geologic evolution and growth history of the interpreted platform structures, together with the depositional and geological processes influencing platform development.

Chapter 4: Results

The Pliocene-Pleistocene study interval is bounded below by sequence boundary SB-PL1 (Sanchez, 2011) and above by the modern seafloor. A second sequence boundary (SB-PL2; Sanchez, 2011) overlies the buried platform 1. The ages of sequence boundaries SB-PL1 and SB-PL2 are insufficiently constrained because of limited sampling at available wells, but Cathro (2002) and Moss et al. (2004) used existing and developed foraminiferal zone analyses to assign ages to both surfaces of 3 Ma or younger.

Sanchez (2011) defined six seismic flat-topped (carbonate) platform packages mainly using seismic facies attributes (Fig.1.4). Sanchez (2011) also recognized asymmetric bidirectional progradation, suggesting that individual platforms prograded greater distances (20-25 km with foreset inclinations of ~7°) to the southwest from than to the northeast (9-15 km with foreset inclinations of up to ~30°). This study, in addition to analyzing internal seismic facies and foreset asymmetry, uses the full capability of the 3D data by mapping high-amplitude platform-top reflections across the their lateral extents.

These platform-top reflections display surface irregularities on both profile views and maps. Platform tops dip << 1° basinward (NW). Sub-seafloor depths to the interpreted tops of buried platforms 1-3 are calculated assuming an average sonic velocity for assumed platform carbonates of ~4000 m/s (Sanchez, 2011; Anselmetti & Eberli, 1993). The platform-top reflections truncate underlying reflections and are onlapped by younger reflections. This allows the relative ages of the platforms to be defined; what we term platform 1 is the oldest, while platform 4 is the youngest (Fig. 1.5).

The platform areas quoted in the descriptions below are defined by the maximum basinward extent of the most recent prograding clinoform foreset within each platform. The landward (SE) platform edges are in turn defined by the locus of initiation of basinward prograding clinoforms. Reflection amplitude maps at different travel-time slices also help to define platform margins. One advantage of 3D seismic data is that the directions of profile slices can be selected to display such prograding clinoforms optimally. As noted by Sanchez (2011), basinal progradation is greater to the SW (18km) than to the NE (8-13 km).

Platform 1

Platform 1, the oldest one mapped, is located in the northeastern part of the Dampatch 3D survey area (Fig. 3) and is, onlapped by the Platform 2 sequence boundary (Fig. 4.1a). The depth to the interpreted platform top varies from 247 m to 398 m (232 ms – 372 ms) below the modern sea surface.

Platform 1 is characterized by continuous internal reflections; such reflections in the extreme SW are more discontinuous and have more variable amplitudes, which may in part be caused by merging two different 3D seismic volumes with different resolution (Figure 4.1b) High-amplitude, progradational reflections comprise the most prominent facies. The progradation is three-dimensional: Figs 4.1a and 4.1b illustrate progradation to the W-NW and SW, respectively.

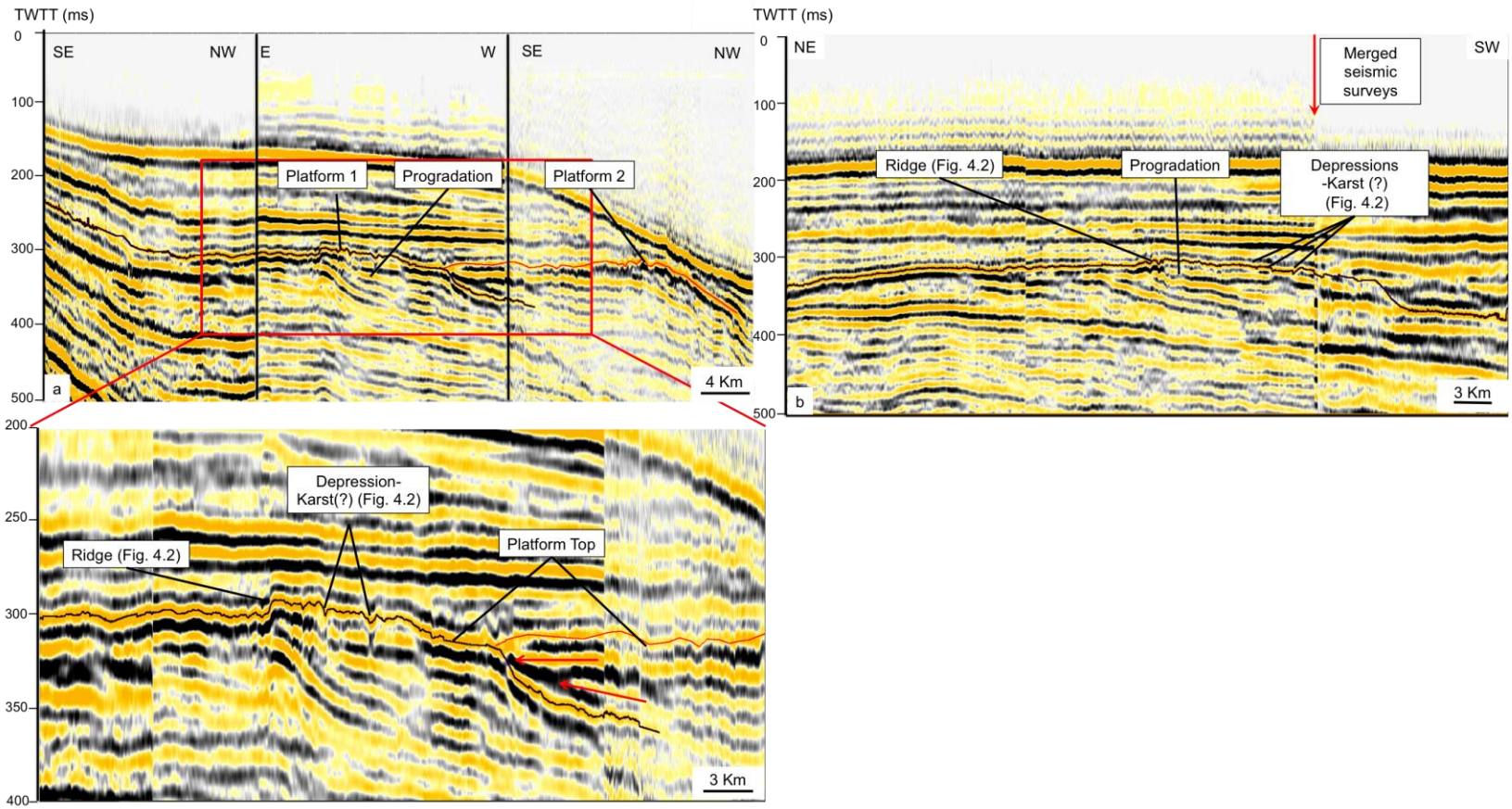

Figure 4.1: Seismic stratigraphic development and facies relationship between platform 1 and platform 2. (a) Showing mapped extents of platform tops. Lower panel: Enlarged image shows depressions (karst?) and onlap of platform 2 against platform 1. Both platform tops are diagnostic of sequence boundaries. The position of a lineated topographic feature that crosses the platform 1 top is also shown (see Fig. 4.2). See Fig. 3 for profile location. (b) Strike-oriented (NE-SW) seismic profile through platform 1 showing internal facies changes, from continuous progradational reflections within the NE part of the platform to discontinuous, variable amplitude reflections to the SW. This profile also crosses the lineated topography highlighted in Fig. 4.2. See Fig. 3 for profile location

The platform top area is ~1100 km^2 (Fig. 4.2) and its basinward progradation distance ranges from 8 to 13 km. A NW-SE oriented linear ridge, prominent in map view, is ~11 km long and ~3 km wide (labeled 2 on Fig. 4.2*)*. The lineated feature appears to be a ridge formed by outcropping of one of the prominent prograding clinoforms. W to E directed progradation eroded on the western side appears to create this topographic high (Fig. 4.1a).

The platform top is an irregular sequence boundary (Figs. 4.1 and 4.2). Seismic profiles show that observed irregularities are v-shaped depressions, up to ~40 m deep and ~1 km wide (Figs. 4.1a and 4.1b). A mapped horizon slice shows that all of the depressions occur in clusters (labeled 3 and outlined by white lines, Fig. 4.2). They do not display linear trends parallel to the mapped platform (paleo-shelf) edge, making them appear different from those mapped by Cathro and Austin (2001). Highs occur close to the SW margin of the platform, and range from 750-850 m in width and 20 - 30 m in height (labeled 4, Fig. 4.2).

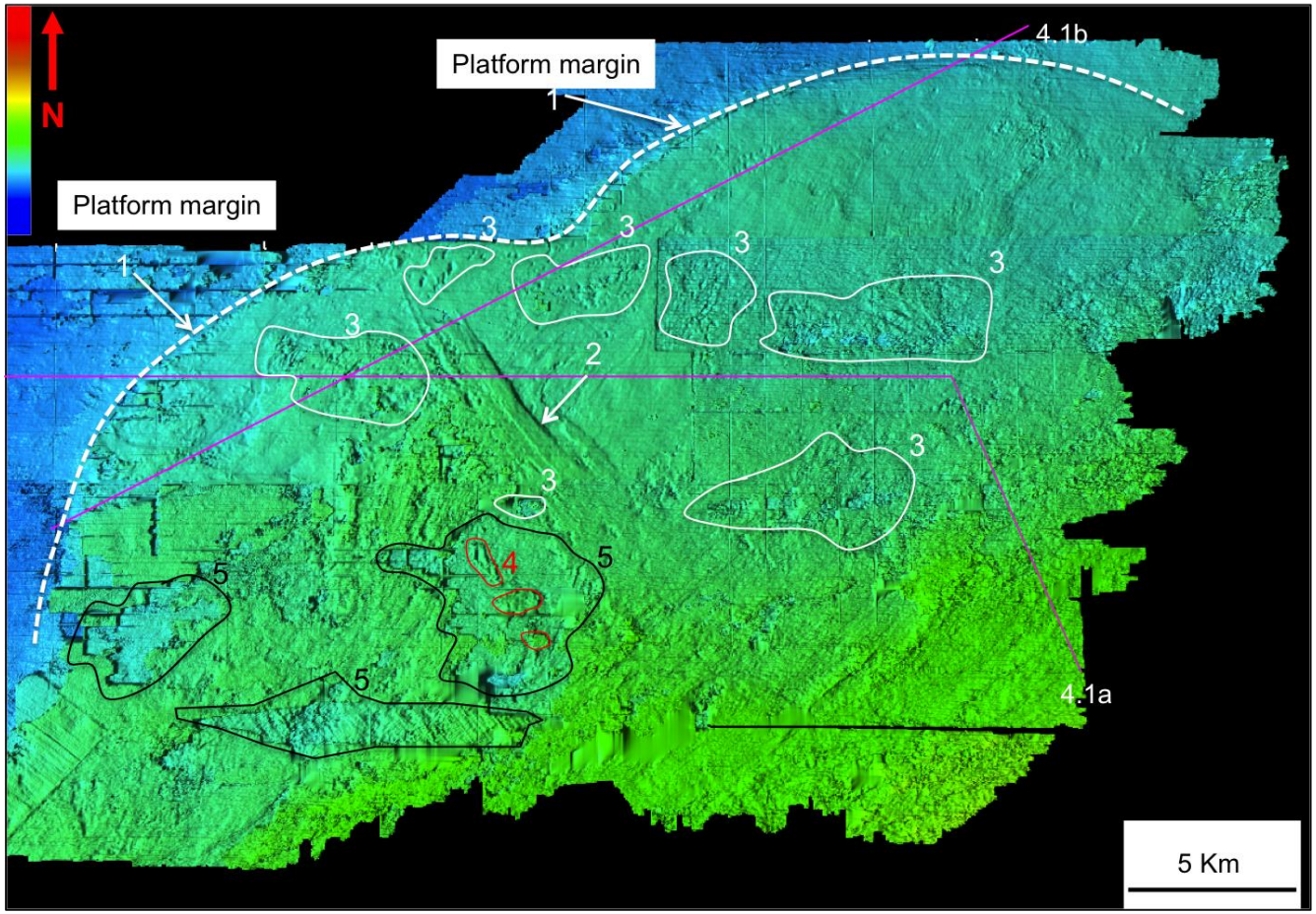

Figure 4.2: Map of the interpreted top of platform 1. The lobate mapped margin is labeled 1. This surface represents a sequence boundary characterized by numerous irregularities (labeled 3). A lineated topographic feature ~11 km long (labeled 2) and oriented NW-SE crosses the platform (see also Figs. 4.1a, b). A number of topographic highs (labeled 4) and artifacts (labeled 5) are also evident. See text for detailed description.

Other apparent depressions are clearly artifacts caused by merging 3D volumes with different acoustic character (labeled 5 and outlined in black, Fig. 4.2). These features cannot be identified as artifacts based on the map view alone, but their outlines and distribution can be observed by migrating through multiple time slices vertically.

Platform 2

Platform 2 is located in the southern part of the Banambu 3D survey area, and the northwestern part of the Dampatch 3D survey area (Fig. 3). This platform is the most basinward of the four platforms interpreted. The depth of the platform top below the sea surface varies from 364 m to 396 m (319 ms –397 ms). Platform 2 covers an area of ~180 km^2. Progradation is mainly to the NW; the distance between the oldest and most recent prograding clinoforms indicates a progradation distance of ~16 km (Fig. 4.3a). Clinoform rollover positions in profile views illustrate progradation trajectories (Steel and Olsen, 2002). The oldest rollover is at 353 ms. The subsequent shelf-edge trajectory is gently rising to rollovers at 347 ms and 332 ms. The trajectory then falls from 332 ms to 348 ms (Fig. 4.3a).

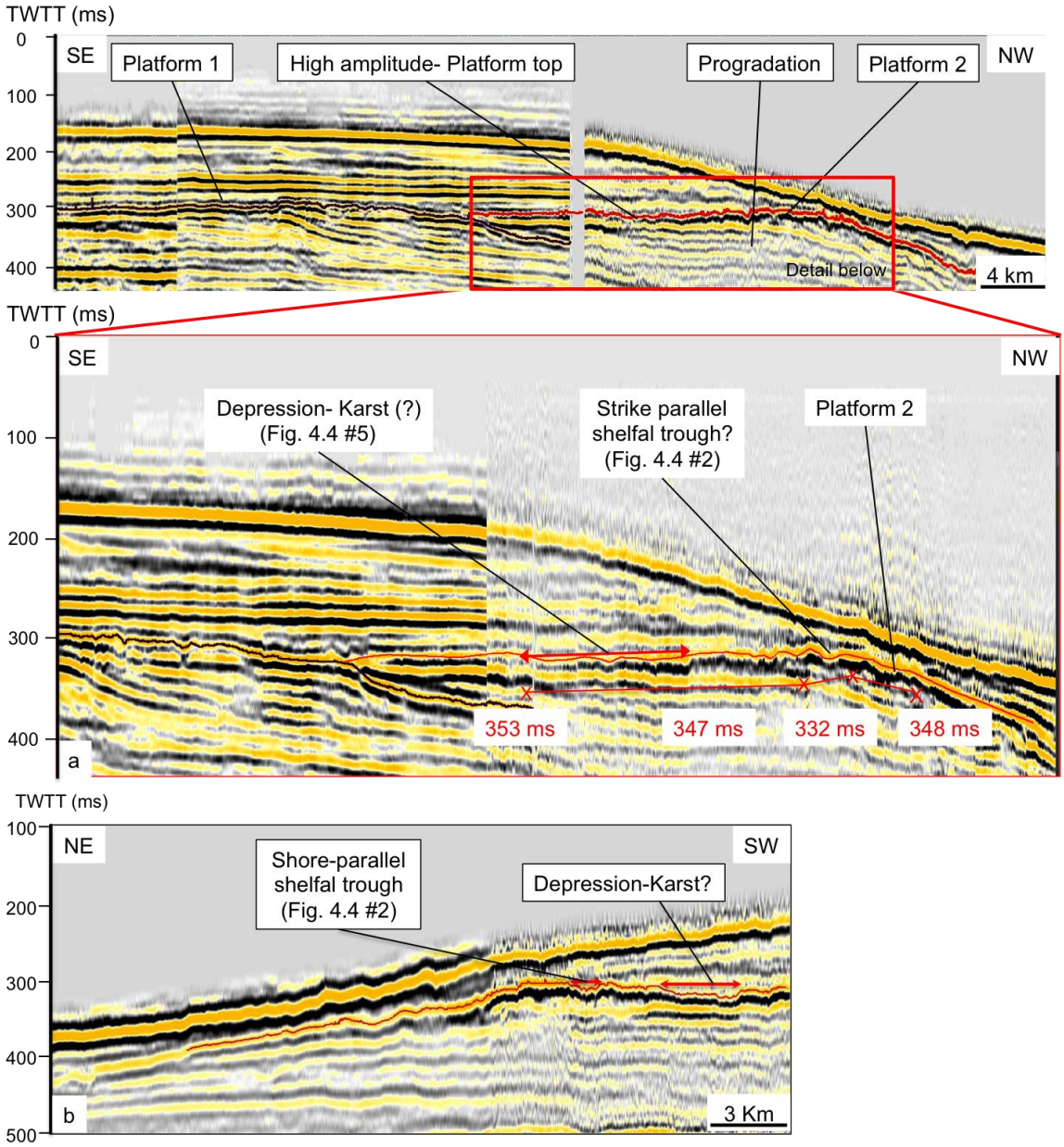

Figure 4.3: Upper panel: Platform 2, showing facies relationship with platform 1. a) Interpreted enlargement, showing both depressions (karst?) and the cross-section of a strike-parallel trough that are associated with truncation of underlying reflections.

Figure 4.3: (Continued) Such truncation, together with onlap against the platform top reflection, indicate that this platform top is a sequence boundary, as is also true of the top of Platform 1. Red crosses show clinoform rollover positions to illustrate progradation trajectories; the oldest rollover is at 353 ms and the subsequent trajectory is gently rising to rollovers at 347 and 332 ms. The trajectory then falls to 348 ms. Such a trajectory indicates progradation followed by forced regression (Steel and Olsen, 2002). See Fig. 3 for profile location. (b) Strike- oriented (NNE-SSW) seismic profile showing seismic facies associated with Platform 2, together with irregularities on the platform top representing a strike-oriented shelf parallel trough and a depression that may be karst (see Fig. 4.4). The red line is the high-amplitude reflection platform top interpreted as a sequence boundary. Internal reflections within the platform are generally of lower amplitude. See Fig. 3 for profile location

U- to V-shaped, strike-parallel, channel-like troughs, ~40 m deep and 700-1000 m wide, incise the high-amplitude platform top (Figs. 4.3a, 4.3b, 1 and 2, Figs. 4.4). Two troughs are identified on platform 2, each consisting of linear to arcuate segments. Both trend NW -SW, orthogonal to the direction of clinoform progradation. The shorter trough (1, Fig. 4.4) is 5.3 km long and the longer trough (2, on Fig. 4.4) is at least 12 km long. Trough 2 has two basinward extensions (3, Figs. 4.4). These amphitheater-shaped extensions are ~1.5 km wide along- strike and extend ~1.8 km basinward of the trough in the dip direction. Other studies have defined similar features of Miocene age on the NWS. For example, Cathro and Austin (2001) mapped a trough composed of three individual segments, each up to 500 m wide and 60 m deep, and with a combined length of ~8 km. Roselff-Soerensen et al. (2012) interpreted two sub-parallel troughs 300-1000 m wide and several kilometers long.

In addition to these troughs, wider, less elongate depressions also occur, mainly on the shallowest, proximal part of platform 2. The depths of these depressions vary from 30-40 m (Figs. 4.3a and b on Fig. 4.4). The northeastern depression (4, Figs. 4.4) is roughly circular, ~5 km in width and covers an area of ~20 km^2. To the south, a more irregularly shaped depression (5, Fig. 4.4) is ~8 km across E-W and ~3.5 km N-S, with an area of 18km^2.

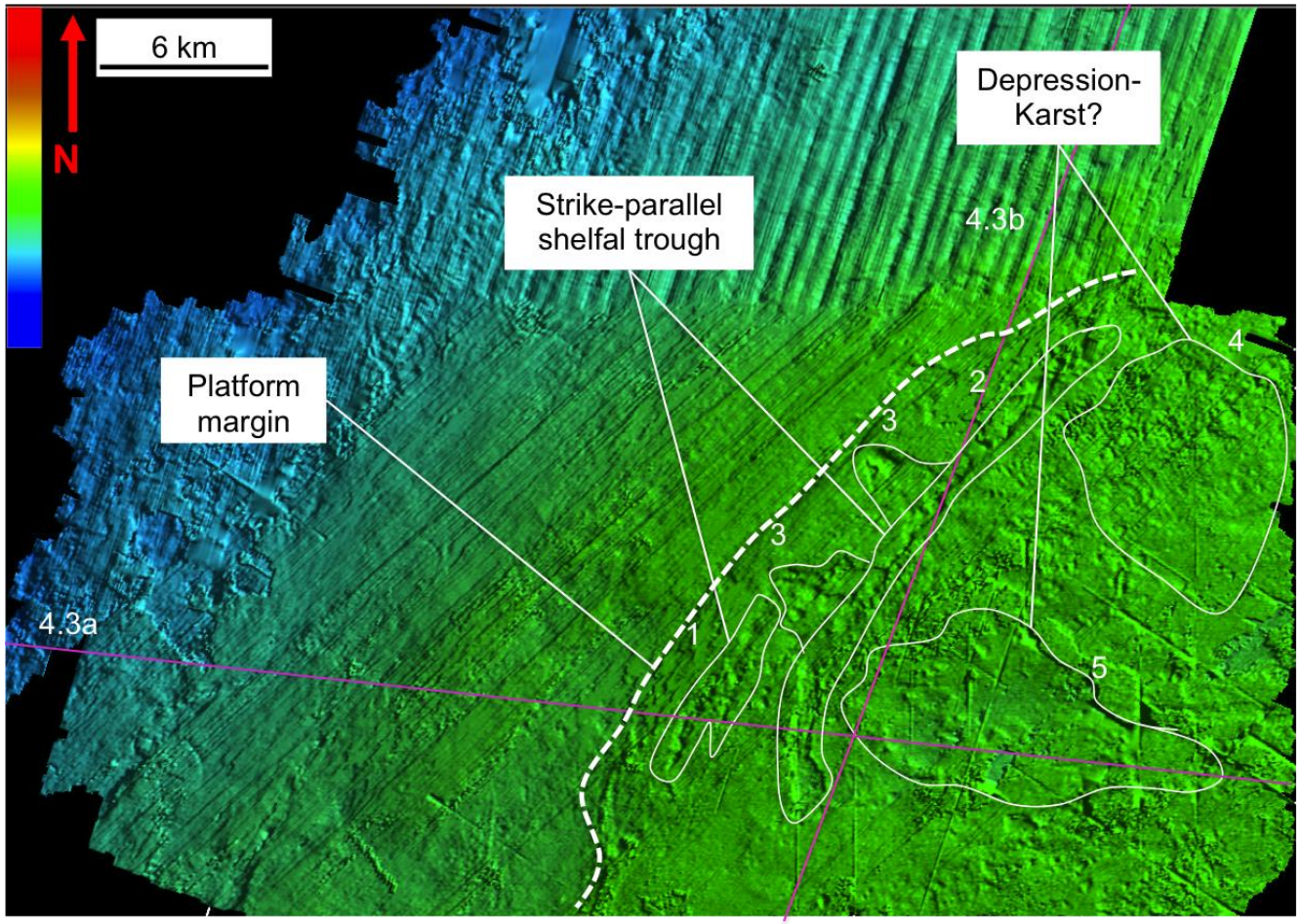

Figure 4.4: Map of the top of Platform 2. The surface is a sequence boundary with many irregularities. Interpretations highlight strike- parallel (SW-NE) troughs (1, 2).

Figure 4.4: (Continued). Amphitheater-shaped extensions (3) occur on the NW (basinward) side of the longer trough and could represent collapse features In addition, there are other irregularities (4, 5) of various size coverage areas are larger than troughs might be karst basin. See text for detailed description

Platform 3

Platform 3 is located within the central Dampatch 3D survey area (Fig. 3). The stratigraphic relationship between platforms 2 and 3 is not as clear as that between platforms 1 and 2. Therefore, it is difficult to confirm that Platform 3 is younger than Platform 2. Fig. 4.5a displays the most direct relationship, showing that the top of both looks like a single reflection, also mapped by Sanchez (2011). However, the portion of the reflection identified as platform 3 is higher, suggesting that it is younger. The depth of the platform 3 top below sea surface varies from 252 m to 349 m (206 ms-377 ms). Platform 3 covers an area of ~ 460 km^2 and its top dips northwest (basinward) at <<1°. The dip of the slope at the platform margin ranges from 2° to 3° (Figs. 4.5c, 4.6).

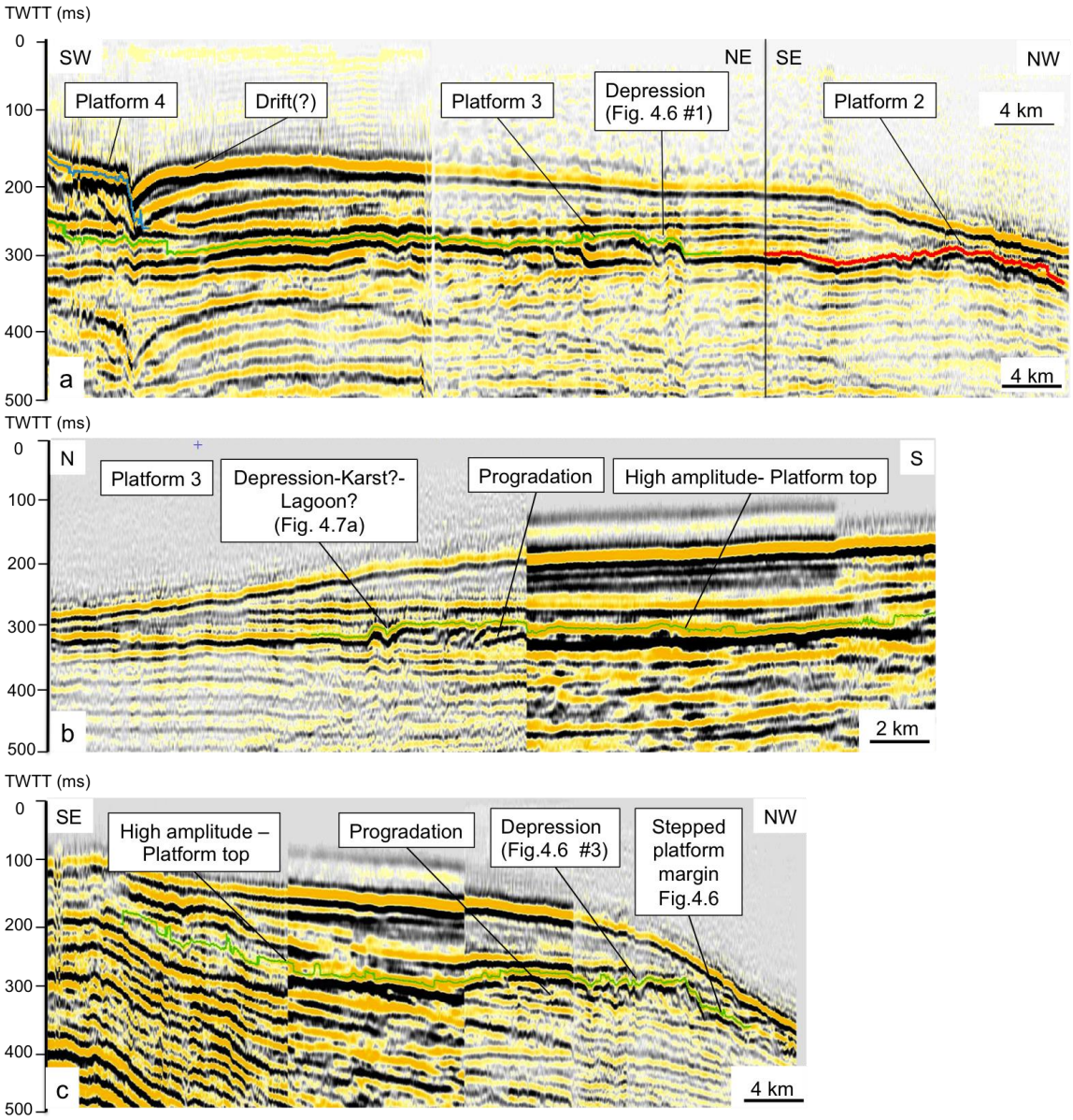

Figure 4.5: (a) Interpreted (SW-NE) seismic profile across Platform 3 and Platform 2, showing the age relationship and progradation to the NE. Note that the same horizon appears to bound both platforms, although the observation that platform 3 is higher than platform 2 suggests that 3 is younger. Onlap and downlap occurs onto the base of Platform 4 by sediments overlying Platform 3. Mounded seismic geometries of these overlying sediments, and the presence of a moat adjacent to Platform 4, suggest that these sediments constitute a sediment drift. See Fig. 3 for profile location.

Figure 4.5: (Continued) (b) Seismic profile showing platform 3 progradation of ~18 km in N direction and depressions (labeled 1 and 2: 25-40 m in depth, 2-13 km in width, see also Fig 4.5a) within the platform top. (c) Interpreted (SE-NW) seismic profile showing the progradation direction of Platform 3, towards the NW, in addition to N and NE, creating this lobate platform. The most recent clinoform foreset is also the steepest (~3°) and represents the platform margin with stepped part which might have developed due to uneven N-NW progradation shown in Fig 4.6

The distance between the oldest and most recent prograding clinoforms within platform 3 indicate platform progradation of ~18 km, principally directed to the N and NW (Figs. 4.5b and c), creating a lobate geometry (Figs 4.6 and 4.7a). This stepped platform margin is also displayed in Fig. 4.5c, and might have developed due to uneven N-NW progradation (Figs. 4.6 and 4.7b). Changing locations of the platform margin in between time slices at 344 ms and 312 ms (a and b, Fig. 4.7c) support the idea of progradation direction changing through time from NW to N, then NE. The oldest rollover is at 308 ms; the rollover trajectory then falls to 318 ms (Fig. 4.7a).

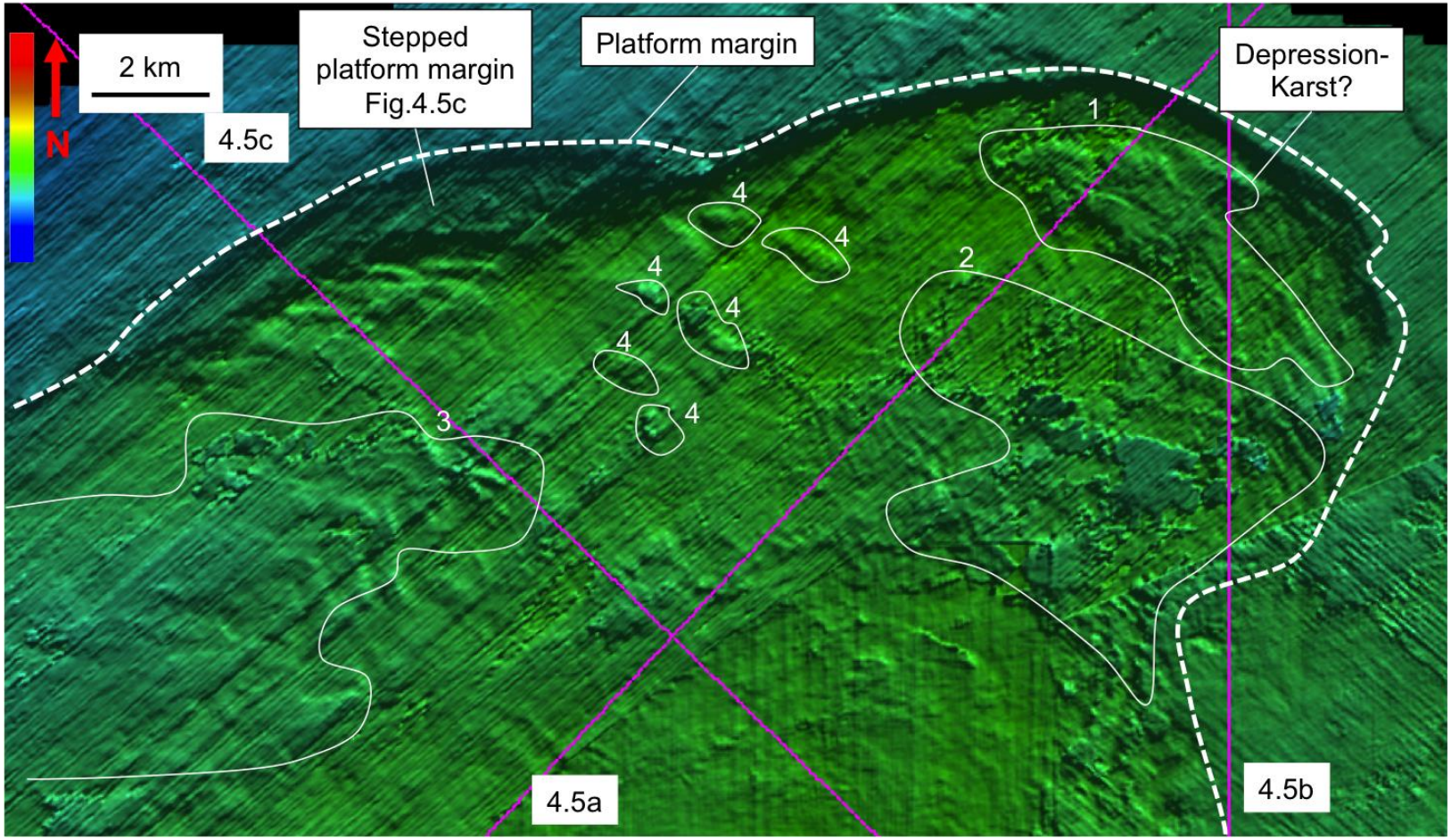

Figure 4.6: Mapped top of Platform 3. This surface represents a sequence boundary, also characterized in part by numerous irregularities. These depressions may represent karst or, particularly with the larger depressions #1, #2 and #3

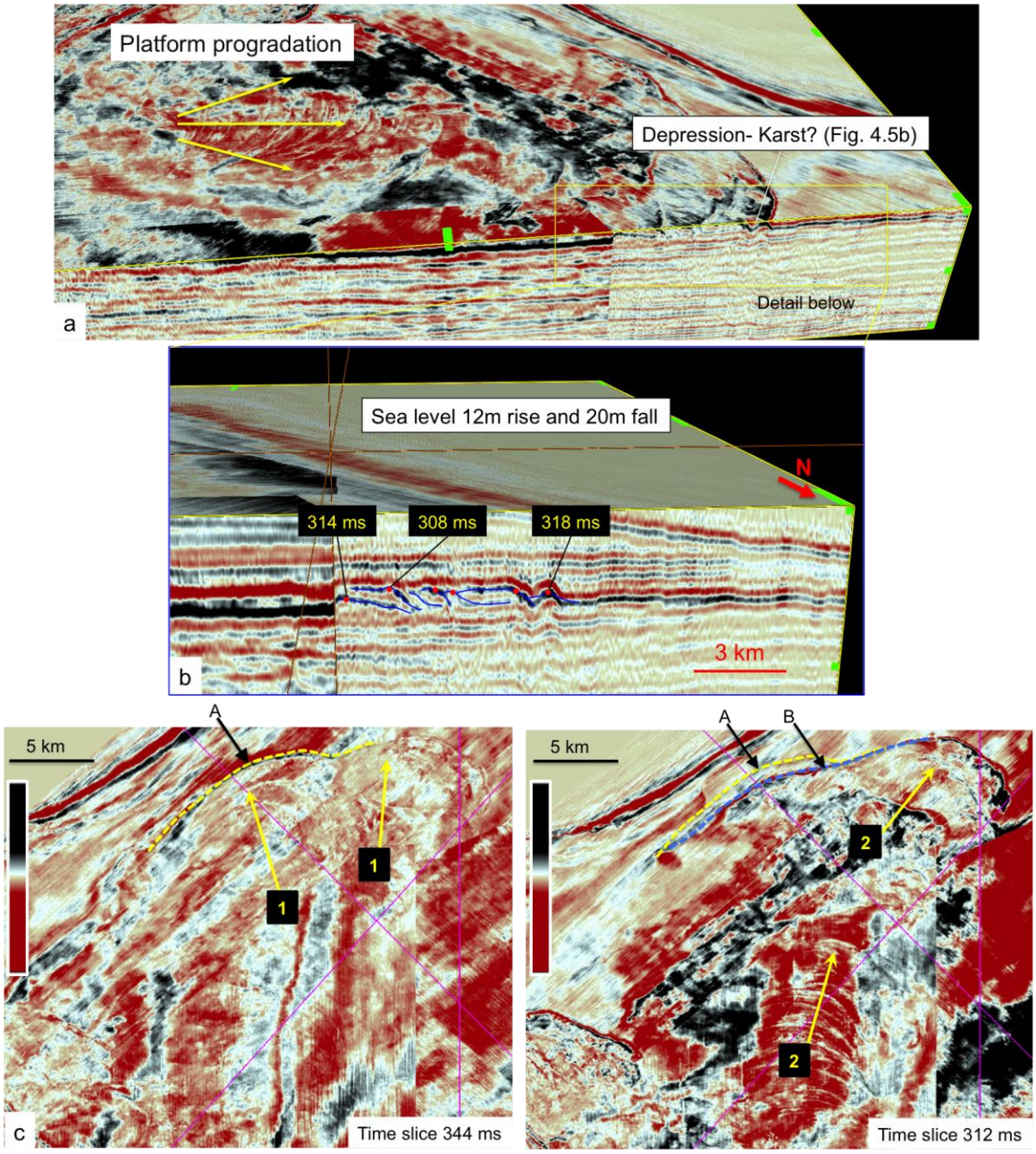

Figure 4.7: (a) Horizontal time slice through Platform 3 at 304 ms with intersecting vertical profile displaying platform-top depressions and prograding clinoforms (see also Fig. 4.8). b) Expanded view of the profile showing clinoforms (in yellow) with highlighting of rollovers at 308 and 318 ms to illustrate falling stage trajectory that must have accompanied a relative sea-level fall (~20 m).

Figure 4.7: (Continued) (c) Time slices at 344 ms and 312 ms, respectively, showing the lobate progradation and its changing orientation through time. Yellow arrows in time slices at 344 ms and 312 ms indicate principal progradation direction, which has changed from N-NW (arrow #1) to NE (arrow #2). Note that changing the progradation direction results in retrograde movement towards the continent (changing the position of platform margin from A to B, shown by black arrow.

Depressions, which truncate underlying reflections, can be identified on the platform top, both on seismic profiles and maps (Figs. 4.5 - 4.6; 1 to 4. See also Fig. 4.7 a). Unlike the troughs on Platform 2, some of which are oriented NE-SW, the depressions on Platform 3 do not display any preferred orientations. The largest depressions (1, 2 and 3 on Figs. 4.6) are 25 - 40 m deep and 2 - 13 km wide. The smaller depressions are ~25-40 m deep, and 0.7-1.5 km wide (labeled 4 on Figs. 4.6). They cover areas ranging from 10 to 50 km^2.

Platform 4

Platform 4 is located within the southwestern Dampatch 3D survey area (Fig. 3), is the youngest of the four mapped platforms, and is the only platform partly exposed at the seafloor. Platform 4 downlaps onto the most basinward extension of platform 3. Fig. 4.8 shows younger sediments, overlying platform 3, that onlap platform 4. These sediments have a mounded architecture; a moat is formed adjacent to Platform 4. Like platforms 1-3, platform 4 contains prograding clinoforms; however, this platform has prograded only ~6.2 km to the NE. However, this distance is a minimum estimate, and not directly comparable with such distances measured for the other platforms, because possible superimposed buildups obscure deeper reflections that may also be progradational (Fig. 4.8a).

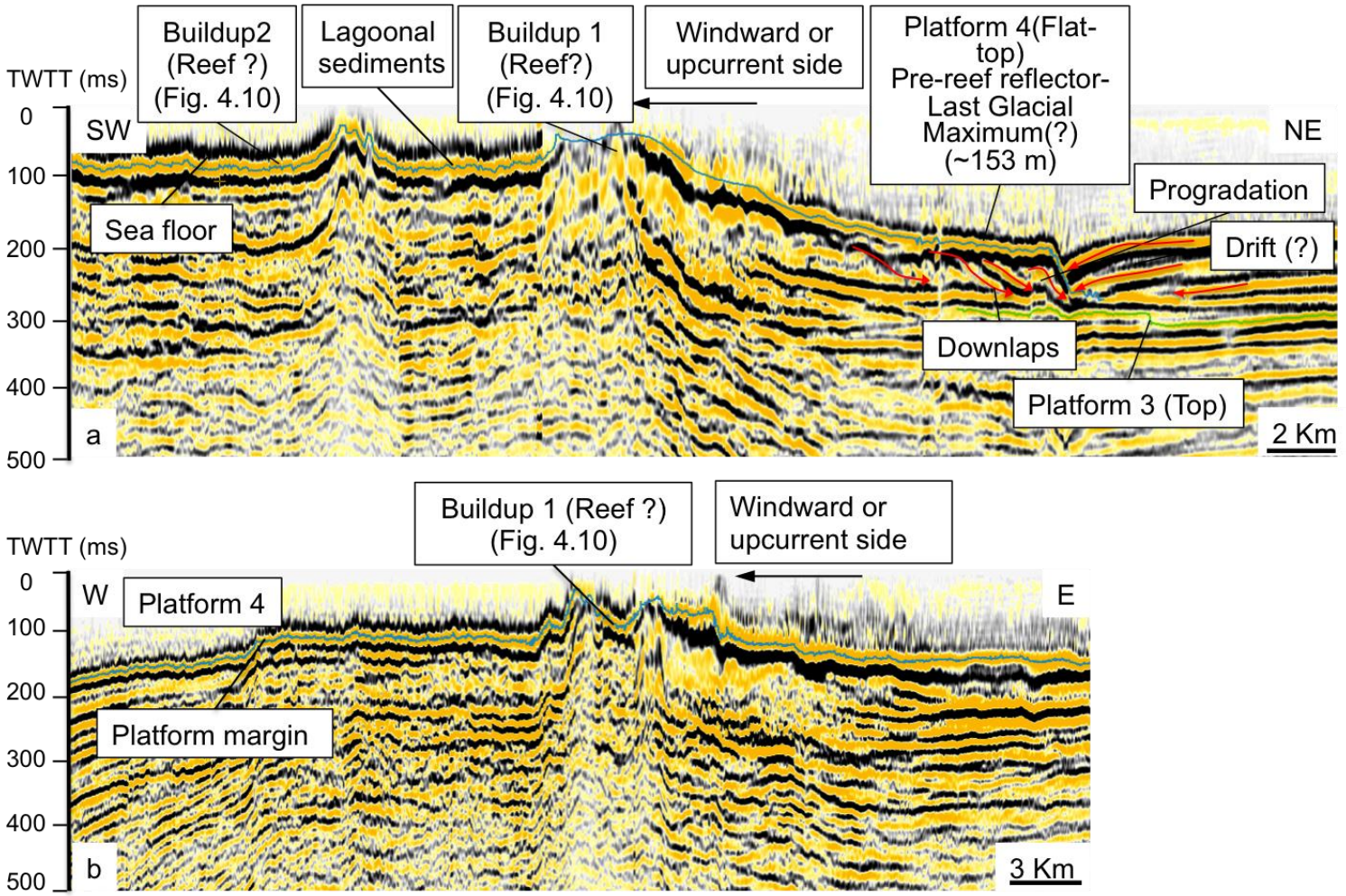

Figure 4.8: (a) Dip-oriented, direction-direction seismic profile crossing Platform 4 showing elevated morphology associated with interpreted reef/bioherm development (reef/bioherm 1 and 2 are shown)

Figure 4.8: (Continued) Light blue horizon located on the top of platform 4 is the modern seafloor. Interpretation shows NE progradation of the platform overlain by reef/bioherm development. The flat top surface marks the top of the progradational platform and highlights the transition to reef/bioherm development, which probably occurred following the Last Glacial Maximum (LGM). Note enhanced reef/bioherm growth to the NE, which we interpret as the windward or upcurrent side (considering the drift features on the platform top, see Fig. 4.10), suggesting high-energy, clear-water, nutrient-rich conditions that promoted reef/bioherm development. Moreover, the observed drift feature (Fig. 4.5a) would be an indicative of the current direction, flowing from Northeast side. (b) Interpreted W-E directed seismic profile of platform 4, reef/bioherm buildup 2, illustrating interpreted elevated topography and chaotic internal reflections representative of such growths. Eastern platform margin is defined by topographic changes

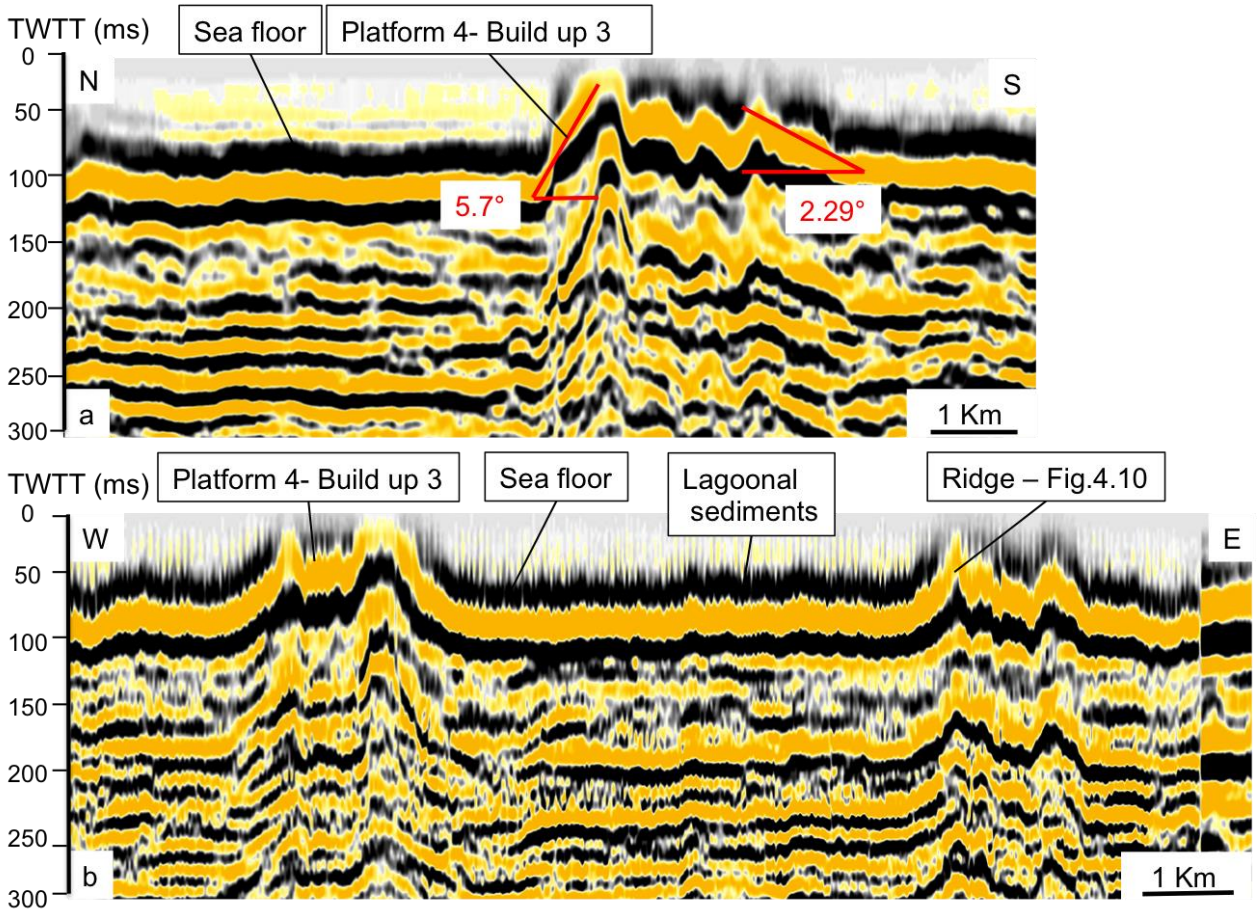

Figure 4.9: (a) N-S directed seismic profile crossing buildup 3, platform 4, showing different elevations on both sides. (b) W-E directed profile crossing the same buildup 3 and other ridges, displaying slightly different dips on each side. See also Fig, 4.10.

Unlike those older platforms, platform 4 has undergone a second phase of development involving superposition of localized buildups, consisting of lower amplitude and chaotic reflections top the prograding clinoforms (Figs 4.8 and 4.9). These topographic highs are exposed at the seafloor and lie at water depths of only 9-19 m (12-25 ms). The depth of the superimposed topographic highs below the sea surface varies from 9 m to 158 m (12 ms to 210 ms). The depth below the sea surface of the remainder of the top of platform 4's prograding clinoforms ranges from 149 m - 158 m (199 – 210 ms) (Fig. 4.8a). The platform covers an area of 505 km^2 (Fig. 4.10).

Part of the high-amplitude platform top is coincident with the modern seafloor. Below the sea floor, lower amplitude, chaotic and discontinuous internal reflections truncate higher amplitude, prograding, internal reflections (Fig. 4.8a). The foresets that prograde over the most basinward part of platform 3 constitute the earliest stage of development of Platform 4. Progradation within platform 4 is mainly to the N-NE, in contrast to the earlier platforms, which prograde mainly to the N-NW. Although much of the platform top is obscured, unlike platforms 1-3 there are no U- and V-shaped irregularities on top of the prograding clinoforms of platform 4.

The top of observed localized buildups at 12 m (16 ms), 19 m (25 ms) and at 9m (12 ms) below the modern sea surface are mapped in detail (Fig. 4.11a). Buildup 1 is ~3 km wide in the W-E direction and ~6 km wide in the N-S direction, covering an area of ~18 km^2 (Fig. 4.10a). Buildup 2 is developed to the SW side of buildup 1, is roughly circular (Figs. 4.10a), and has an area of 2.5 km^2 and a width of 1.4 km. Buildup 3 developed to the S of buildup 2, and is ~ 4 km wide in N-S direction and 5.5 km in W-E direction (Fig. 4.11a). Another buildup right next to buildup 3 appears to consist of prolonged sediment ridges (Figs 4.9b and 4.10). A time slice at 48 ms shows both circular and arcuate features defined as buildups and ridges.

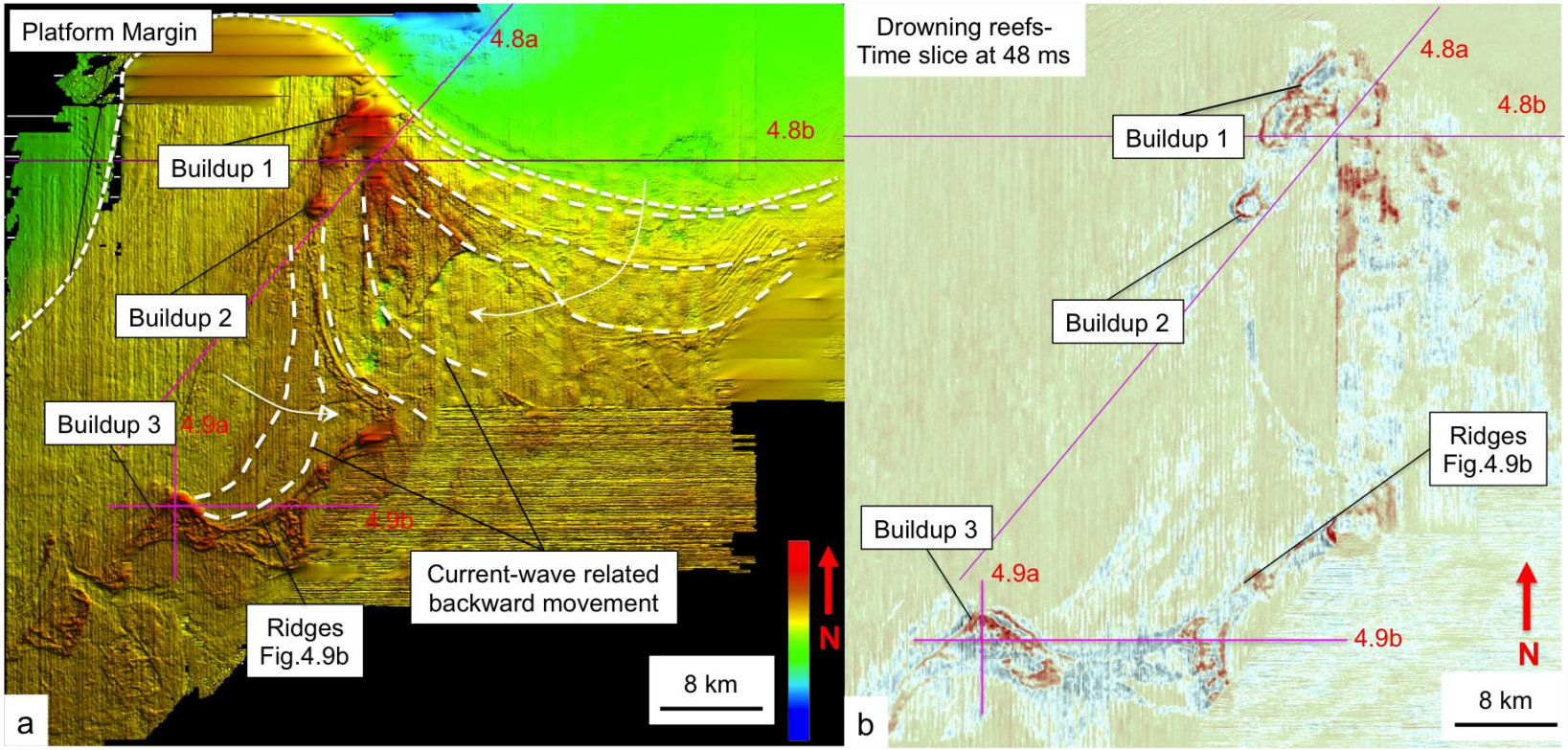

Figure 4.10: (a) Seafloor map showing the top of Platform 4 and interpreted circular-shaped reefs/bioherms. Note apparent migration of arcuate ridges in various directions (mainly towards the SW on the northern side and towards the E on the western part of the platform. (b) Enlarged time slice at 48 ms showing circular shapes interpreted as reefs/bioherms and positions before they (presumably) drowned. Profile views 4.8 and 4.9 crossing these interpreted reefs/bioherms. Labeled reefs/build-ups are 13km^2, 2.5km^2 and 12 km^2 in area, respectively. The observed arcuate ridges suggest shaping of unconsolidated sediments by waves and/or currents.

Figure 4.10: (Continued) The location of these ridges appears to migrate in space, which indicates that the direction of the controlling mechanism (currents?) has also changed through time. White dashed lines indicate arc-shaped ridges and the arrows highlight their SW movement on the NE side of the platform and SE movement on the SW side

The bases of the buildups cannot be identified due to their chaotic, mounded, discontinuous, internal reflections. Their edges tend to be elevated, their NE slope has generally greater relief (Figs. 4.8a and 4.10a.). In contrast, buildup 2 has similar dips on both sides (Fig. 4.8b). Unlike buildups 1 and 2, buildup 3 displays steeper sides (Fig. 4.9a). The seafloor map suggests that these topographic highs may have initiated as separate buildups, which later became connected by arcuate ridges (Fig. 4.10a). The most characteristic features of these observed arcuate ridges (Fig. 4.10a and b) are their arrhythmic pattern and the tendency of one ridge to parallel the adjacent one. Migrating through multiple time slices vertically, it is clear that one ridge set migrates towards the S-SW, while the other set migrates to the E. Buildup 1 lies at the western end of the first ridge set, buildup 2 is located at the northern end of the second set, and buildup 3 is located on the southern end of the second set.

Chapter 5: Discussion

We interpret the observed progradational seismic packages, topped by high-amplitude, ~flat, sequence bounding reflections as tropical carbonate platforms built by photozoan organisms (e.g., bioherms; Schlager, 1998). The platform tops are very gently dipping (<<1°) and distally steepen on their slopes to 2°-4°, leading to their classification as "flat-topped" carbonate platforms (Read, 1985; Sanchez, 2011). Such morphologies are observed worldwide, notably on the Australian Great Barrier Reef, the South Florida shelf, and in the Bahamas. Clinoforms within each platform mapped on the NWS record progradation to the NW, N and NE, in all cases towards the paleo shelf-edges, creating lobate morphologies (Fig. 1.5).

The NWS platforms overlie interpreted NW-prograding middle Miocene Bare Formation delta lobes; these lobes migrated NE along margin strike with time (Sanchez, 2011). In contrast, the platforms migrate from NE to SW (Fig. 1.5). Sanchez (2011) has attributed this SW migration either to differential rates of tectonic subsidence influenced by the Banda Arc collision to the north or to differential compaction of the underlying clastic depocenters (Collier, 1989; Schmoker and Gautier, 1989). Such differential compaction may be due to juxtaposition of sediment units with different compositions and diagenetic potentials during highstands and lowstands along depositional strike; this has been observed in the Bahamas (Eberli, 2002).

The ages of the platforms are poorly constrained, but the sequence boundaries capping the platforms are Pliocene-Pleistocene in age, as estimated by Sanchez (2011) and based on Moss et al., (2004) (Figs. 4.1, 4.3, 4.5 and 4.8).

The growth of carbonate platforms anywhere, is controlled by initial topography, differential subsidence at regional to local scales, tectonic activity (faulting, tilting and

local folding), eustasy, climate, and the type of carbonate production, which is highly sensitive to terrigenous and nutrient inputs (Longman, 1980; Hallock, 1988; Montaggioni, 2000). In addition, glacio-eustatic control and/or episodic tectonism can generate meter-scale cycles that shape carbonate production (Fournier et al., 2005). Ocean currents, climatic factors and wind circulation can also influence platform morphology by reworking and redepositing sediment and through their effects on nutrient levels and water temperatures supporting photozoan carbonate primary productivity (Pomar et al., 2001; Vecsei, 2004), though these effects can be difficult to recognize (Fournier et al., 2005). Besides shaping the morphologies of the platforms, changes in these multiple controls are also responsible for reductions in platform growth rates and their ultimate demise (Kendrick et al., 1991). In particular, relative sea-level falls contribute to termination of shallow-water carbonate production through exposure of platform tops, leading to erosion and karstification. We investigate the roles of these factors on the development of the NCB carbonate platforms mapped seismically for this investigation

Platform Initiation

Heterozoan carbonate sedimentation dominated on the NWS until interrupted by the middle Miocene siliciclastic influx that became the Bare Formation (Apthorpe, 1988). Delta lobes of the Bare Formation provided a shallow-water setting and topographic highs that fostered carbonate platform growth after the siliciclastic influx terminated during the Pliocene (Sanchez, 2011; Sanchez et al., 2012a; 2012b). Meanwhile, continued northward drift of the Indo-Australian Plate had moved the NCB from ~40° S in the Oligocene - Miocene (Veevers et al., 1991) to its present (tropical) location at ~20° S (McGowran et al., 2004). Resulting warmer sea-surface temperatures, coupled with a shelfal substrate within the photic zone, favored photozoan carbonate production

(Kendalland and Schlager, 1981) in the Pliocene (Veevers et al., 1991; McGowran et al., 2004).

The NCB has therefore experienced fundamental sedimentological transitions during the middle Miocene-Pliocene, from heterozoan carbonates to siliciclastics and finally to photozoan carbonate production (Cathro, 2002; Liu et al., 2011; Sanchez, 2011; Sanchez et al., 2012a; 2012b). A similar evolution in sedimentation has occurred in the Browse Basin to the NE (Rosleff-Soerensen et al., 2012). In the Browse Basin, the transition was from a non-tropical ramp in the Eocene-Miocene to a tropical rimmed platform in the middle Miocene. An intervening siliciclastic influx is not observed. This transition has been attributed in part to the strength of the warm-water LC along the Australian west coast (Rosleff-Soerensen et al., 2012). The LC at present is up to 100 km wide and flows SW along the NWS in water depths <300 m (Pattiaratchi, 2004). Its initiation and strength are related to evolving connectivity through the Indonesian Seaway and high sea-surface temperatures in the West Pacific Warm Pool (WPWP; Gallagher et al., 2009; Sinha et al., 2007). Rosleff-Soerensen et al. (2012) have inferred that the Browse Basin was the southern limit of tropical reef development on the NWS during the Miocene (Rosleff-Soerensen et al., 2012), and also the southernmost extent of the LC influence at that time (Collins et al., 2006). However, transpressional reactivation of the Mermaid Fault during the early stages (middle Miocene) of the collision between the Indo-Australian and Eurasian plates at the Banda Arc created topographic highs that may have permitted reef development farther south, e.g., Rowley Shoals (Ryan et al., 2009). Topographic highs (relief up to 75 m) also occur in the Rosemary-Legendre structural trend defined by Cathro and Karner (2006) but platform development has not been observed associated with those features.

Platform Growth

All four platforms have progradational internal geometries (Figs. 4.1, 4.3, 4.5 and 4.8). Therefore, we presume that the primary process controlling their growth is production of clastic carbonate sediment on platform tops and deposition in deeper water accommodation space beyond ambient and evolving seaward platform margins. Framework (reef) building photozoan organisms, if present at all, must be minor components of the platforms until the final phase of the development of platform 4 (see below). This is in contrast to persistent patch reef development in the adjacent Browse Basin (Rosleff-Soerensen et al., 2012). Measured progradation distances within platforms 1-3, 8, 16 and 18 km, respectively, increase with decreasing platform age. A smaller measured progradation distance, 6,2 km, for platform 4 breaks this trend, but this distance represents a minimum, because chaotic reflections beneath inferred buildups on top of this platform obscure what could be older prograding clinoforms (Fig. 4.9a). This increase in progradation distance for more recent, and more SW, platforms was interpreted by Sanchez (2011) as a spatial relationship between the underlying siliclastic (delta lobe) depocenters and the overlying platforms. Delta lobes, producing subtle topographic highs, then control both initiation and position of the ensuing shallow-water tropical carbonate/platform system (Fig. 1.4). The oldest platform developed above the youngest siliciclastic lobe (Sanchez, 2011). Perhaps younger platforms, prograding into reduced (shallower-water) accommodation space, had to prograde farther in basinward directions. Complex, lobate prograding relationships also might be associated with shifts in the trend of the LC).

Progradation trajectories are well imaged only for platforms 2 (Figs. 4.3a) and 3 (Fig. 4.7b). Both platforms display a transition from a gently rising progradational trajectory to a forced regressive trajectory that suggests a rise followed by a fall in

relative sea level. The best imaged profile for trajectory analysis within platform 2 exhibits a 30 m rise followed by a 32 m fall (Fig. 4.3a). In platform 3, the equivalent trajectory components suggest a 12 m rise followed by a 20 m fall (Figs. 4.7b). Moreover, changes in principal progradation direction from N-NW (platforms 1-3: Fig 4.7c) to N-NE (Platform 4; Fig. 4.8a) may signal a change in the strength of oceanographic mechanisms (waves and currents) controlling platform morphologies. This change appears to have occurred during the growth of platform 3, which experienced a change in progradation direction from NW to N-NE (Fig. 4.7c).

Interpreted seismic profiles and mapped horizon slices all reveal differences in platform top morphology among the four mapped platforms that are, at least in part, related to their progradation histories. For example, the 11 km long by 3 km wide lineated topography on platform 1 is unique (Figs. 4.1a, b and 4.2). Seismic profiles indicate that this feature is a ridge created by outcrop of the upper part of one of the prograding clinoforms within the platform. It is possible that growth of platform 1 through progradation during a relative sea-level rise was interrupted by a subsequent sea-level stillstand or minor fall, indicated by the lower elevations of subsequent clinoforms (Fig. 4.1a). The changing sea levels, and potential associated subaerial exposure, may have allowed cementation and creation of the observed erosion-resistant ridge. Similar ridges (the largest up to 17 km in length) have been identified in the Miocene of the Browse Basin and are proposed to be the first true tropical reef build-ups (Rosleff-Soerensen et al., 2012). The platform 1 ridge, however, does not readily fit a reef interpretation, because of the continuity of underlying reflections and the absence of chaotic reflections. Several topographic highs also occur in the southern part of platform 1 (Figs. 4.2). These highs are more irregular than the ridge. We suggest that their origins are related to relative sea-level stillstands or falls, possibly coupled with varying levels of

external (wind, wave and/or current) energy acting on the platform as it evolved. Part of the difference in image quality between the SW and NE halves of the platform 1 top surface map (Fig. 4.2) arises because 3D surveys of different degrees of seismic resolution, within the Dampatch merged survey, are merged within the mapped area of platform 1 (Fig 4.1b)

Analogous ridges and other topographic highs do not occur on younger platforms 2 and 3. However, on platform 4, arc- shaped (sediment) ridges of a seismically very different appearance connect interpreted reef buildups. We interpret these ridges, oriented ~perpendicular to the presumed predominant along-strike current direction (NE to SW) as sediment waves (Fig 4.10). According to Off (1963), rhythmic linear sand body heights exceeding 25 feet in the North Sea are caused by tidal currents which develop perpendicular to the predominant current direction. These features are discussed further below in connection with platform 4.

Exposure of Platform Tops

U- and V-shaped troughs (40 m deep and ~1 km wide) and broader depressions (~25 – 40 m deep and 2-13 km wide) occur on all platform tops except platform 4. These troughs and depressions truncate underlying reflections (Figs. 4.1, 4.3 and 4.5) and therefore incise the high-amplitude platform-top reflections. The depressions outlined by black lines and labeled 5 on Fig. 4.2 are in fact artifacts in a low-resolution component of the merged 3D volume.

The evolution of platform 4 differs markedly from that of platforms 1-3 in that we do not believe that platform 4 has undergone an exposure phase. On platform 4, overlying buildups obscure much of its underlying progradational component (Fig. 4.8).

Strike-parallel troughs, each up to 700-1000 m wide and 40 m deep on platform 2 near its basinward margin (labeled 1 and 2, Fig. 4.4), resemble shelfal troughs described by Cathro and Austin (2001) near paleo-shelf edges of early mid-Miocene clinoforms; their troughs are each up to 500 m wide and 60 m deep. Cathro and Austin (2001) have interpreted these features as karst formed as a consequence of preferential dissolution along shelf-edge-parallel lithological heterogeneities during shelf exposure. Roselff-Soerensen et al. (2012) have also reported similar troughs on the early middle Miocene barrier reef in the Browse Basin which are 300-1000 m wide and several kilometers long; they also have interpreted these troughs as karst.

More circular-like depressions in platforms 1 (#3, Fig. 4.2), 2 (#4 and 5, Fig. 4.4) and 3 (#4, Fig. 4.6) are ~25-40 m deep and 0.7-5 km in width. We can compare these depressions with similar circular features mapped by Cathro et al. (2003), ~76 m deep and 170-250 m wide in Oligocene-Miocene and early middle Miocene sequence boundaries. Rosleff-Soerensen et al. (2012) have also defined a feature ~2200 m in diameter, a prolongation of one of their interpreted troughs, which they interpreted as a classic doline. Other similar examples of depressions identified on 2D and 3D seismic data occur in the Miocene of the Gippsland Basin offshore southeastern Australia (Brown, 2004). These circular depressions, seismically identified and 200-500 m in diameter are interpreted as sinkholes. Irregular depressions interpreted as extensive near-vertical karst collapse chimneys with diameters ranging from 150-915 m also occur in Ordovician carbonates of the Ellenburger Formation in the Fort Worth Basin of north-central Texas (Hardage et al., 1996).

We therefore interpret the NCB platform-top incisions in platforms 1-3 as karst, likely formed as a result of subaerial exposure by relative sea-level falls. Troughs located on platform 1 (labeled 3, Fig.4.2), and clustered depressions on platform 3 (labeled 1 and

2, Fig. 4.6) are more irregularly shaped, but we also interpret them as karst. The generally high amplitudes of the platform-top reflections (Figs. 4.1, 4.3 and 4.5), which contrast with generally lower amplitude internal reflections, may also imply cementation associated with meteoric diagenesis caused by subaerial exposure.

Reef/Bioherm Development

Reef/bioherm development did not occur everywhere or immediately after Bare Formation siliclastic input ceased. We observe no seismic evidence of reef-like buildups on platforms 1-3 (Figs. 4.2, 4.4 and 4.6), which are instead progradational, suggesting purely clastic depositional/erosional processes. However, platform 4 (Fig. 4.10) underwent a second phase of development, involving superposition of localized buildups composed of lower amplitude and chaotic reflections, on top of an earlier progradational edifice (Fig. 4.8a). We interpret these buildups as reefs/bioherms. Since there is no evidence of topographic highs caused by faulting on the progradational base of platform 4, formation of these reefs must have been driven by relative sea-level change and/or a changing oceanographic (more than currents) regime, either or both of which could have influenced photozoan carbonate productivity (Betzler, et al., 2009). Between interpreted reef/bioherm buildups, we interpet intervals of more continuous reflections as lagoonal and/or hemipelagic sediments (Fig.4.8a). Reef/bioherm development shifted progressively landward, as can be observed (Fig 4.10a marked by white arrow) by moving through the 3D seismic volume vertically in travel time; such time slice views reinforce the hypothesis of such a shift being a response to continuously rising relative sea level.

The long-term history of reef development in the NCB is not well documented. Seismic evidence for buildups is limited. Liu et al. (2011) speculated that some Miocene

seismic buildups in the NCB, ~160 m diameter and ~500 m by 1300 m in diameter might have been reefs. Cathro et al., (2002) also observed one isolated middle Miocene mound, with dimensions of 1200 m by 2000 m and ~80 m of relief. So besides some Browse Basin (Rosleff-Soerensen et al., 2012) and Dampier Basin buildups, observations of reef development in the NWS are intermittent. Ryan et al. (2009) and Collins et al. (2002) did observe rare reefs in the Pliocene- Quaternary section up to 28°S.

During the LGM, widespread shelf exposure occurred over the NWS (Fairbanks, 1989; Fleming et al., 1998; Wyrwoll et al., 2009). The top of prograding clinoforms that form the base of Platform 4 currently lie at ~153 m below the sea surface (Fig. 4.8a), suggesting that the platform was near sea level at the LGM. According to Gurnis et al. (2009) sudden drowning of reefs along the passive margin of the Marion Plateau off northeastern Australia has been explained deepening topography due to dynamic subsidence, which caused the rate of relative sea level rise to outpace global sea level rise 11 -7 Ma. In the Maldives archipelago, atoll crests are carbonate ridges, subaerially exposed and eroded during the last sea level minimum (Anderson, 1998). Since 50-60 Ma, Maldivian atoll basement has subsided ~2000 m, suggesting an average subsidence rate of ~3-4 cm ky^{-1} (Anderson, 1998). In the NCB buildups began to form at a depth today of ~153 m, in the photic zone at or near the LGM. Further analysis of their post-LGM development will require along-strike subsidence modelling and knowledge or the compaction rate of underlying siliciclastic deposits.

Buildup 1 exhibits strongest growth towards the N-NE, where the relief of the reef is highest. This direction faces the paleoshelf edge and into the presumably SW-flowing LC (Fig. 4.8a). Mounded sediments onlapping the progradational base of platform 4 from the NE, where a moat (Fig. 4.8a) is also present, resemble younger drift deposits. We conclude that a current was active around the platform during development of buildup 1.

Similar moats are observed on the Marion Plateau, northeast Australia, and are there also interpreted as contourites (Isern et al., 2004; Betzler et al., 2009; Fig.4.8a). Buildup 2 is more symmetrical (Fig. 4.8b), but buildup 3 is asymmetric, with a steeper N flank and a more gently sloping S flank (Fig. 4.9a). Such differences in orientation and flank dips suggest control by oceanographic mechanisms acting in defined directions.

On the top of Platform 4, arcuate sediment ridges connect the buildups (Fig. 4.10a). Similar features are interpreted as reefs by Rosleff-Soerensen et al., (2012) in the early middle Miocene section of the Browse Basin. Platform 4 ridges appear to have migrated W to SW along strike (white arrow, Fig. 4.10a), What appear to be relict ridges are concave to the N, and appear as arcs to the E of the most recent ridge (white dashed lines, Fig. 4.10a). Such apparent migration may be further evidence of the persistent influences of currents and waves on platform 4 development.

Platform Demise

The four mapped platforms formed successively, migrating in a generally SW direction, as noted by Sanchez (2011). Onlap relationships suggest that the older platform was terminated before the next platform was initiated. Such a relationship is, however, difficult to confirm for the transition between platforms 2 and 3 (Fig. 4.3a). Two possible explanations for such successive carbonate platform termination are drowning by a sufficiently rapid relative sea-level rise and/or subaerial exposures by cyclical relative sea-level falls (Schlager, 1989). Evidence for subaerial exposure in the form of interpreted karst features on the tops of platforms 1-3 implies that these platforms were all terminated by such relative sea-level falls.

The basal, progradational base of platform 4 may also have terminated during the eustatic fall prior to the LGM, although karst has not been identified on platform 4.

However, the presence of younger reef/bioherm buildups on top of the progradational base indicates a different subsequent history from that of platforms 1-3. We presume that these buildups formed during the rapid, post-LGM eustatic rise. The reefs/bioherms are possibly not active today, although the buildups remain exposed at the seafloor. We suggest that drowning must also have been the mechanism for termination of observed reef/bioherms of platform 4. However, under ideal conditions, reefs are capable of keeping up with any conceivable rate of relative sea-level rise (Schlager et al. 1989). So, deterioration in environmental conditions necessary for growth must also have been involved. For example, sediment carried by currents and deposited as observed drift deposits may have inhibited reef growth (Betzler et al., 2009; Davies, 1991; Isern et al., 2004; Fig.4.8a). The composition of the sediment comprising these drifts is unknown, but the associated turbidity would have hindered primary carbonate production. (Erlich et al., 1990; Betzler et al., 2009).

Leeuwin Current

The LC, driven by the Indonesian Throughflow (ITF) from the WPWP, has been often defined as an important environmental factor in the initiation of platform/ reef development. Reef development extension expanded to 29°S (the Houtman-Abrolhos reefs; Zhu et al., 1993) by the LC during the late Pleistocene. Observed buildups on platform 4 might also record trends of the LC. Tectonic reconstruction and restriction of the ITF suggest a weaker LC at 3.3-3.1 Ma; surface layer cooling until 2.4 Ma is also observed. This may have been associated with the mid- Pliocene global cooling of 2-3°C at ~3.3 Ma (Sinha et al., 2007; Karas et al., 2011). After 2.4 Ma, with the intensification of trade winds, the NWS remains relatively warm, without strong coastal upwelling. However, weakening and strengthening of the LC would be expected within each

Pleistocene glacial/interglacial cycles (most recently with periods of 10^5 y.). Generally lower sea surface temperature (SST) occur since the last interglacial ~125Ka (Wyrwoll et al., 2009) Conversely, at the LGM (21 Ka) lower sea level results in reduced LC activity along the NWS. The onset of LC after LGM investigated by James et al, (2004). He used the absence of ooid formations from 15.5 -12.7 Ka to infer a reduction in LC strength, after which the LC strengthened. Drill cores compiled from Houtman-Abrolhos coral reefs (Collins et al., 1993) suggest reef accumulation from 13 Ka onward, supporting such renewed LC activity. This may also have promoted reef development on platform 4. Overall, the observed succession of carbonate platforms sitting over Bare Formation siliciclastics, with their subaerially exposed tops, suggest activation of LC at 2.4 Ma, but with fluctuation intensity in response to glacial/interglacial cycles. However, conditions suitable for reef development within the survey area did not occur until after the LGM, possible at ~13 Ka.

Chapter 6: Conclusion

Interpretation of 3D seismic data has revealed the detailed morphologies of four well-defined Plio-Pleistocene flat-topped carbonate platforms. Progradational platforms are capped by rugged platform tops with subtle geomorphologies that allows us to understand platform development. Progradational internal seismic facies indicate sufficient carbonate sediment supply to fill available accommodation space. All four platforms feature similar progradational platform geometries, but the youngest platform, platform 4, is unique in featuring superimposed buildup geometries, interpreted as reefs, and onlapping sediment drift deposits.

- Platform 1-4 are low-angle, warm-water carbonate platforms with steeper platform margins on their NE-N-NW side, presumed to be facing upcurrent. Mapped high-amplitude platform-top horizons reveal interpreted karst development on all platforms except platform 4.
- Buildups observed on platform 4 are connected with ridges. Reef (bioherms) initiation at 153 m was within the photic zone at the LGM (sea level ~130 m below present level; removal of subsidence, possibly dynamic, would bring the reefs closer to LGM sea level) suggesting that reef development was post-LGM.

Current effects may have been stronger on platform 4 than on earlier platforms. This is indicated by sediment drift deposits which occurred after the sea-level fall that terminated the progradational base of platform 4. Migrating arcuate ridges suggest the wind and current energy were the principal during the most recent time period.

References

Anderson, R. C. (1998). Submarine topography of Maldivian atolls suggests a sea level of 130 metres below present at the last glacial maximum. *Coral Reefs*, *17*(4), 339–341. doi:10.1007/s003380050135

Anselmetti, F. S., & Eberli, G. P. (1993). Controls on sonic velocity in carbonates. *Pure and Applied Geophysics PAGEOPH*, 141(2-4), 287–323. doi:10.1007/BF00998333

APTHORPE, M. (1988) Cainozoic depositional history of the North West Shelf. In: The North West Shelf Australia: Proceedings of Petroleum Exploration Society (Ed. by P.G. Purcell & R.R. Purcell), pp. 55–84. PESA, Perth.

BERGGREN, W.A., KENT, D.V., SWISHER, C.C., III & AUBRY, M.-P. (1995) A revised Cenozoic geochronology and chronostratigraphy. In: Geochronology, Time Scales and Global Stratigraphic Correlations: A Unified Temporal Framework for an Historical Geology (Ed. by Berggren W.A., Kent D.V., Aubry M.-P. & Hardenbol J.), Society of Economic Paleontologists and Mineralogists Special Volume 54, 129–212.

Betzler, C., Hübscher, C., Lindhorst, S., Reijmer, J.J.G., Römer, M., Droxler, A., Furstenau, J., Ludmann, T. (2009). Monsoon-induced partial carbonate platform drowning (Maldives, Indian Ocean). Geology 37, 867-870.

BRADSHAW, M.T., YEATES, A.N., BEYNON, R.M., BRAKEL, A.T., LANGFORD, R.P., TOTTERDELL, J.M. & YEUNG, M. (1988) Paleogeographic evolution of the North West Shelf region. In: The North West Shelf Australia (Ed. by P.G. Purcell & R. R. Purcell), Proceedings North West Shelf Symposium, Perth, pp. 29–54.

Brown, A. R. (2004). Interpretation of Three-Dimensional Seismic Data, AAPG Memoir 42. American Assoc.Petr. Geol. (9). doi:10.1190/1.9781560802884

Butcher, B. P. (1989). Northwest Shelf of Australia. AAPG Special Publications .

CATHRO, D.L. & AUSTIN, J.A. Jr. (2001) An early mid-Miocene, strike parallel shelfal trough and possible Karstification in the Northern Carnarvon Basin, Northwest Australia. Mar. Geol., 178, 157–169.

Cathro, D. L. (2002). Three-Dimensional Stratal Development of Carbonate- Siliciclastic Sedimentary Regime, Northern Carnarvon Basin, Northwest Ausrtalia. Dissertation Thesis, The University of Texas at Austin, Austin, Texas

Cathro, D. L., Austin, J. A., Moss, G. D. (2003). Progradation along a deeply submerged Oligocene – Miocene heterozoan carbonate shelf : How sensitive are clinoforms to sea level variations ?, *10*(10), 1547–1574.

Cathro, D. L., & Karner, G. D. (2006). Cretaceous–Tertiary inversion history of the Dampier Sub-basin, northwest Australia: Insights from quantitative basin modelling. *Marine and Petroleum Geology*, *23*(4), 503–526. doi:10.1016/j.marpetgeo.2006.02.005

Catuneanu, O., Galloway, W. E., Kendall, C. St. G. C., Miall, A. D., Posamentier, H. W., Strasser, A., & Tucker, M. E. (2011). Sequence Stratigraphy: Methodology and Nomenclature. *Newsletters on Stratigraphy*, *44*(3), 173–245. doi:10.1127/0078-0421/2011/0011

Collier, R.E.L. (1989) Modelling the role of differential compaction and tectonics upon Westphalian facies architecture in the Northumberland Basin: Occasional Publication Yorkshire Geological Society, v. 6, p. 189-199.

COLLINS, L. B. (2002) Tertiary Foundations and Quaternary Evolution of Coral Reef Systems of Australia's North West Shelf. In: KEEP, M; MOSS, S.J., (Ed). The Sedimentary Basis of Western Australia 3. In: PETROLEUM EXPLORATION SOCIETY OF AUSTRALIA SYMPOSIUM, Perth, WA. Proc. p. 129-152.

COLLINS, L. B.; ZHAO, J-X.; FREEMAN, H. (2006) A high precision record of mid-late Holocene sea-level events from emergent coral pavements in the Houtman Abrolhos Islands, southwest Australia. Quater. Intern. v. 145/146, p. 78-85.

Colpaert, A., Pickard, N., Mienert, J., Henriksen, L. B., Rafaelsen, B.& Andreassen, K. (2007). 3D seismic analysis of an Upper Palaeozoic carbonate succession of the Eastern Finnmark Platform area, Norwegian Barents Sea. *Sedimentary Geology*, *197*(1-2), 79–98. doi:10.1016/j.sedgeo.2006.09.001

Davies, P. J., J. A. McKenzie, A. Palmer-Julson, et al. (1991), Proceedings of the Ocean Drilling Program, Initial Reports: Ocean Drilling Program, Texas A&M University, College Station, Texas, v. 133, 810 p.

Davies, P.J., Cartwright, J.A., Stewart, S.A., Lappin, M. and Underhill, J.R. (2004) 3D Seismic Techbnology: Application to the Exploration of Sedimentary Basins. Geological Society, London, Memoirs, 29.

DiCaprio, L., Muller, R. D., & Gurnis, M. (2010). A dynamic process for drowning carbonate reefs on the northeastern Australian margin. *Geology*, *38*(1), 11–14. doi:10.1130/G30217.1

Eberli, G.P., Anselmetti, F.S., Kroon, D., Sato, T. and Wright, J.D. (2002) The Chronostratigraphic significance of seismic reflections along the Bahamas Transect. Marine Geology. 185, 1-17

Erlich, R.N., Barrett, S.F., Ju, G.B., 1990. Seismic and Geologic characteristics of drowning events on carbonate platforms. AAPG Bulletin 74, 1523-1537.

Exon, N.F. and Colwell, J.B. (1994) Geological history of the outer North West Shelf of Australia: a synthesis. AGSO J. Geol. Geophys., 15, 177–190

Fairbanks, R.G. (1989). A 17,000-year glacio-eustatic sea level record: influence of glacial melting dates on the Younger Dryas event and deep ocean circulation. Nature 342, 637–642.

Fleming, K., Johnston, P., Zwartz, D., Yokoyama, Y., Lambeck, K., & Chappell, J. (1998). Refining the eustatic sea-level curve since the Last Glacial Maximum using far- and intermediate-field sites, *163*, 327–342.

Fournier, F., Borgomano, J., & Montaggioni, L. F. (2005). Development patterns and controlling factors of Tertiary carbonate buildups: Insights from high-resolution 3D seismic and well data in the Malampaya gas field (Offshore Palawan, Philippines). *Sedimentary Geology*, *175*(1-4), 189–215. doi:10.1016/j.sedgeo.2005.01.009

Gallagher, S. J., Wallace, M. W., Li, C. L., Kinna, B., Bye, J. T., Akimoto, K., & Torii, M. (2009). Neogene history of the West Pacific Warm Pool, Kuroshio and Leeuwin currents. *Paleoceanography*, *24*(1). doi:10.1029/2008PA001660

Hardage, B. A., Carr, D. L., Lancaster, D. E., Simmons, J. L., Elphick, R. Y., Pendletonfl, V. M., & Johns, R. A. (1996). 3-D seismic evidence of the effects of carbonate karst collapse on overlying clastic stratigraphy and reservoir compartmentalization, *61*(5), 1336–1350.

Hallock, P. (1988). The role of nutrient availability in bioerosion: consequence to carbonate buildups. Palaeogeography, Palaeoclimatology, Palaeoecology 63, 275–291

HEATH, R.S. & APTHORPE, M.C. (1984). New formation names for the late Cretaceous and Tertiary sequence of the Southern North West Shelf. West. Australia Geol. Survey Record 1984/7.

Hull, J N F., Griffiths, C. M. (2002). Sequence stratigraphic evolution of the Albian to Recent section of the Dampier Sub-basin , North West Shelf Australia, 617–639.

Isern, A. R., Anselmetti F. S., Blum. P. (2004). A Neogene Carbonate Platform, Slope, and Shelf Edifice Shaped by Sea Level and Ocean Currents, Marion Plateau (Northeast Australia). *AAPG Memoir 81,* 291-307.

James, N. P., Bone, Y., Kyser, T. K., Dix, G. R., & Collins, L. B. (2004). The importance of changing oceanography in controlling late Quaternary carbonate sedimentation on a high-energy, tropical, oceanic ramp: north-western Australia. *Sedimentology*, *51*(6), 1179–1205. doi:10.1111/j.1365-3091.2004.00666.x

Karas, C., Nürnberg, D., Tiedemann, R., & Garbe-Schönberg, D. (2011). Pliocene Indonesian Throughflow and Leeuwin Current dynamics: Implications for Indian Ocean polar heat flux. *Paleoceanography*, *26*(2), PA2217. doi:10.1029/2010PA001949

Karner, G. D., & Driscoll, N. W. (1999). *Style, timing and distribution of tectonic deformation across the Exmouth Plateau, northwest Australia, determined from stratal architecture and quantitative basin modelling*. *Geological Society, London, Special Publications* (Vol. 164, pp. 271–311). doi:10.1144/GSL.SP.1999.164.01.14

Kendall, C., G. and Schlager, W. (1981). Carbonates and relative changes in sea level, Marine Geology, *44*, 181–212.

KENDRICK, G.W., WYRWOLL, K. - H., AND SZABO, B.J., 1991, Pliocene–Pleistocene coastal events and history along the western margin of Australia: Quaternary Science Reviews, v. 10, p. 419–439.

Liu, C., Fulthorpe, C. S., Austin, J. A., & Sanchez, C. M. (2011). Geomorphologic indicators of sea level and lowstand paleo-shelf exposure on early–middle Miocene sequence boundaries. *Marine Geology*, *280*(1-4), 182–194. doi:10.1016/j.margeo.2010.12.010

Longley, I. M., & Bradshaw, M. T. (2001). AUSTRALIAN PETROLEUM PROVINCES OF THE TWENTY - FIRST CENTURY, AAPG Memoir, 74, 287–317.

Longman, M. (1980). Carbonate diagenetic textures from near-surface diagenetic environments. Am. Assoc. Pet. Geol. Bull., 64: 461-487.

Masaferro, J., Bourne, R., Jauffred, J. (2003). 3D visualization of carbonate reservoirs. *The Leading Edge*.

McGowran, B., Li, Q., Cann, J., Padley, D., McKirdy, D. M., & Shafik, S. (1997). Biogeographic impact of the Leeuwin Current in southern Australia since the late

middle Eocene. *Palaeogeography, Palaeoclimatology, Palaeoecology*, *136* (1-4), 19–40. doi:10.1016/S0031-0182(97)00073-4

McGowran, B., Holdgate, G.R., Li, Q., Gallagher, S.J., 2004. Cenozoic stratigraphic succession in southeastern Australia. Australian Journal of Earth Sciences 51, 459-496.

MILLER, K.G.,WRIGHT, J.D. & FAIRBANKS, R.G. (1991) Unlocking the Ice House; Oligocene-Miocene oxygen isotopes, eustasy, and margin erosion. J. Geophys. Res., 96, 6829–6848.

Montaggioni LF (2000) Postglacial reef growth. C R Acad Sci Paris Earth Planet Sci 331:319–330

Moss, G. D., Cathro, D. L., & Austin, J. A. (2004). Sequence Biostratigraphy of Prograding Clinoforns ,Northern Carnarvon Basin , Western Australia : A Proxy for Variations in Oligocene to Pliocene Global Sea Level ?, *19*(3), 206–226.

Mulder, T. and Syvitski, J.P.M (1995) Turbidity currents generated at river mouths during exceptional discharges to the world oceans. The Journal of Geology, 103. 285-299

Off, T. (1963) Ryhtmic Linear Sand Bodies Caused By Tidal Currents. Bulletin of the American Association of Petroleum Geologists.47(2). 324-341

Pattiaratchi, C. (2004). Surface and sub-surface circulation and water masses off Western Australia, Bulletin of the Australian Meterolgical and Oceanographic Society, *19, 95*.

Pomar, L. (2001), Types of carbonate platforms: a genetic approach: Basin Research, v.13, p. 313-334.

Read, J.F. (1985), Carbonate Platform Facies Models: The American Association of Petroleum Geologists Bulletin, v. 69, p. 1-21.

ROMINE, K.K., DURRANT, J.M., CATHRO, D.L. & BERNARDEL, G. (1997) Petroleum play element prediction for the cretaceoustertiary basin phase, northern Carnarvon Basin. APPEA J., 37, 315–339.

Rosleff-Soerensen, B., Reuning, L., Back, S., & Kukla, P. (2012). Seismic geomorphology and growth architecture of a Miocene barrier reef, Browse Basin, NW-Australia. *Marine and Petroleum Geology*, *29*(1), 233–254. doi:10.1016/j.marpetgeo.2010.11.001.

RYAN, M.C., HELLAND-HANSEN, W., JOHANNESSEN, E.P. & STEEL, R.J. (2009) Erosional vs. accretionary shelf margins; the influence of margin type on deepwater sedimentation; an example from the Porcupine Basin, Offshore Western Ireland. Basin Res., 21, 676–703.

Sanchez, C. (2011). Controls on Sedimentary Processes and 3D Stratigraphic Architecture of a Mid-Miocene to Recent , Mixed Carbonate-Siliciclastic Continental Margin : Northwest Shelf of Australia, Dissertation Thesis, The University of Texas at Austin.

Sanchez, C. M., Fulthorpe, C. S., & Steel, R. J. (2012a). Middle Miocene-Pliocene siliciclastic influx across a carbonate shelf and influence of deltaic sedimentation on shelf construction, Northern Carnarvon Basin, Northwest Shelf of Australia. *Basin Research*, *24*(6), 664–682. doi:10.1111/j.1365-2117.2012.00546.x

Sanchez, C. M., Fulthorpe, C.S.,& Steel, R.J. (2012b). Miocene shelf-egde deltas and their impact on deepwaer slope progradation and morphology, Northwest Shelf of Australia. Basin Research, 23(1-16).

Schlager,W., 1989. Drowning unconformities on carbonate platforms. In: Crevello, P.D., Wilson, J.L., Sarg, J.F., Read, J.F. (Eds.), Controls on Carbonate Platform and Basin Development. Special Publication, vol. 44. Society of Economic Paleontologists and Mineralogists (SEPM), pp. 15–25.

Schlager, W. (1998). Exposure, drowning and sequence boundaries on carbonate platforms. Special Publs. Int. Ass. Sediment.25, 3-21

Schlager, W. (2005), Carbonate Sedimentology and Sequence Stratigraphy, SEPM Concepts Sedimentol. Paleontol, 8, 200 pp.sensitive are clinoforms to sea level variations ?, *10*(10), 1547–1574.

Schmoker, J.W., and Gautier, D.L., 1989, Compaction of basin sediments; modeling based on time-temperature history: Journal of Geophysical Research, v. 94, p.7379-7386.

SEMENIUK, V. (1996) Coastal forms and quaternary processes along the Arid Pilbara Coast of Northwestern Australia. Palaeogeogr. Palaeoclimatol. Palaeoecol, 123, 49–84.

Sinha, D. K., Singh, A.K. (2007). Surface circulation in the eastern Indian Ocean during last 5 million years : Planktic foraminiferal evidences, Indian Journal of Marine Sciences, *35(3)*, 342–350.

STEEL, R.J. & OLSEN, T. (2002) Clinoforms, clinoform trajectories and deepwater sands. Sequence stratigraphic models for exploration and production: Evolving methodology, emerging models and application histories (CD-ROM): 22nd Annual Gulf Coast Section SEPM Foundation Bob Perkins Research Conference (Ed. by J.M. Armentrout & N.C. Rosen), pp. 367–380. Houston, TX.

Vecsei, A. and Berger, W.H. (2004). Increase of atmospheric CO_2 during deglaciation: Constrains on the coral reef hypothesis from patterns of deposition. Global Biogeochemical Cycles 18: *doi: 10.1029/2003GB002147. issn: 0886-6236*

VEEVERS, J., POWELL, C.M. & ROOTS, S.R. (1991) Review of seafloor spreading around Australia. Aust. J. Earth Sci., 38, 373–389.

VEEVERS, J.J. & POWELL, C.McA, 1984, Dextral shear within the eastern Indo-Australian Plate, in VEEVERS, J.J., (Ed), Phanerozoic Earth History of Australia, Claredon Press, Oxford, 102-103.

Wallace, M. W., Condilis, E., Powell, A., Redfearn, J., Auld, K., Wiltshire, M., Holdgate, G., Gallagher, E. (2003). GEOLOGICAL CONTROLS ON SONIC VELOCITY IN THE CENOZOIC CARBONATES OF THE NORTHERN CARNARVON BASIN , NORTH WEST SHELF , WESTERN AUSTRALIA, APPEA JOURNAL, 1–15.

Wyrwoll, K-H., Greenstein, B. J., Kendrick, G. W., & Chen, G. S. (2009). The palaeoceanography of the Leeuwin Current : implications for a future world, Journal of the Royal Society of the Western Australia, 92: 37–51

Zampetti, V., Schlager, W., Van Konijnenburg, J.-H., & Everts, A.-J. (2004). Architecture and growth history of a Miocene carbonate platform from 3D seismic reflection data; Luconia province, offshore Sarawak, Malaysia. *Marine and Petroleum Geology*, *21*(5), 517–534. doi:10.1016/j.marpetgeo.2004.01.006

Zhu, Z.R., Wyrwoll, K.H., Collins, L.B., Chen, J.H., Wasserburg, G.J., Eisenhauer, A., 1993. High-precision U-series dating of Last Interglacial events by mass spectrometry: Houtman Abolhos Islands, Western Australia. Earth Planet. Sci. Lett. 118, 281–293.

Vita

Pinar Goktas was born in Ankara, in capital city of Turkey. Upon graduation from Ankara Anadolu High School, she enrolled in Hacettepe University in 2004, where she obtained a B.S degree in Hydrogeological engineering. During her undergraduate years, she participated two internship programs in Turkish Petroleum Corporation (TPAO in Turkish). After graduation the Turkish Petroleum Corporation and the Ministry of National Education (MEB in Turkish) awarded Pinar to pursue a M.Sc degree in Geological Sciences in the USA. She obtained her M.sc degree in 2013. After graduation from Jackson School of Geoscience, University of Texas at Austin, she will be employed as a geologist in Turkish Petroleum Corporation in Ankara, Turkey.

Email: pnr2607@gmail.com

This thesis typed by Pinar Goktas